

# Attitude Control of a 3-DoF Quadrotor Platform using a Linear Quadratic Integral Differential Game Approach

---

## Abstract

In this study, a linear quadratic integral differential game approach is applied to regulate and track the Euler angles for a quadrotor experimental platform using two players. One produces commands for each channel of the quadrotor and another generates the worst disturbance based on the mini-maximization of a quadratic criterion with integral action. For this purpose, first, the attitude dynamics of the platform are modeled and its parameters are identified based on the Nonlinear Least Squares Trust-Region Reflective method. The performance of the proposed controller is evaluated for regulation and tracking problems. The ability of the controller is also examined in the disturbance rejection. Moreover, the influence of uncertainty modeling is studied on the obtained results. Then, the performance of the proposed controller is compared with the classic Proportional Integral Derivative, Linear Quadratic Regulator, and Linear Quadratic Integral Regulator. The results demonstrate the effectiveness of the Game Theory on the Linear Quadratic Regulator approach when the input disturbance occurs.

*Keywords:*

Linear Quadratic controller, Differential Game Theory, Quadrotor, 3-DoF Experimental Platform, Attitude Control.

---

## 1. Introduction

Quadrotors, a type of Vertical Unmanned Aerial Vehicle (VUAV), have found diverse applications in investigation, strategic operations, optical sensing, and entertainment. Precise control is crucial for the safe flight of quadrotors in the presence of disturbances. The Attitude Control System (ACS) plays a vital role in regulating the quadrotor's attitude, and the Proportional Integral Derivative (PID) controller has been commonly employed for this purpose in previous studies [1, 5]. However, due to the nonlinearity of the quadrotor dynamics, the PID strategy's effectiveness diminishes in the presence of disturbances and modeling errors.

To address these challenges and enhance the quadrotor's attitude control, various model-based control strategies have been implemented on the ACS. These strategies encompass nonlinear control, intelligent control, optimal control, and robust control approaches.

Nonlinear control methods such as Synergetic Control [8], Feedback Linearization (FBL) [2], Sliding Mode Control (SMC) [16, 26, 18, 9, 23, 29] have been utilized to regulate the quadrotor's Euler angles (roll, pitch, and yaw angles) intelligently.

Intelligent control approaches, including reinforcement learning [14, 17, 27, 25], iterative learning [12], machine learning [10], and fuzzy logic [13], have also been employed to control the attitude of the quadrotor.

Optimal control strategies, such as Linear Quadratic Gaussian (LQG) [30], Linear Quadratic Regulator (LQR) [3], Linear Quadratic Integral Regulator (LQIR) [4], and Model Predictive Controller (MPC) [28, 22], have been applied to generate optimal control commands for the quadrotor.

In the domain of robust control, techniques like  $H_\infty$  control [24, 21],  $\mu$ -synthesis, and Linear Quadratic Regulator Differential Game (LQR-DG) [19] have been used to stabilize the quadrotor's Euler angles, considering worst-case scenarios and mini-maximization of a quadratic criterion, which includes control effort and regulation performance.

In this paper, an LQIR-DG method is implemented real-time on 3-DoF experimental platform of the quadrotor to produce the robust control commands, i.e. rotational velocity of the quadrotor. To this

end, first, the experimental platform of the quadrotor is modeled using the Newton-Euler formulation and its linear state-space form is derived. Then, the parameters of the quadrotor are estimated by matching experimental data with results from the model simulation. In the next step, the proposed controller is implemented on the Arduino Mega2560 board using the embedded coder platform in MATLAB and its performance is investigated in regulation and tracking problems. Moreover, the rejection capability of the input disturbance and modeling error is tested. Finally, a comparison is also performed between the results of classical PID, LQR, and LQIR with the proposed method. The results demonstrate that this method has an excellent performance in the attitude control of the quadrotor platform. A demo video of the results is available online here.

The remainder of this research is organized as follows: Section 2 presents the problem statement. Section 3 outlines the dynamic platform modeling process. The proposed controller architecture is described in Section 4. Section 5 presents the numerical results, and Section 6 concludes the paper. A demo video showcasing the results is available online <sup>1</sup>.

## 2. Problem Statement

The experimental quadrotor platform rotates freely with rotational velocity ( $\Omega_i, i = 1, 2, 3, 4$ ) about its roll, pitch, and yaw axes, according to Figure 1. The angular velocities in the body frame ( $p, q, r$ ) and the Euler angles ( $\phi, \theta, \psi$ ) are measured using an Attitude Heading Reference System (AHRS). The measured states are utilized in the structure of the proposed controller to stabilize the quadrotor platform. The graphical abstract of the LQIR-DG controller strategy is depicted in Figure 2.



Figure 1: 3-DoF Quadrotor platform.

---

<sup>1</sup>Demo video link: [https://drive.google.com/drive/folders/1DIJs3wmIpmpwI8slyHeitA6Ebe-khKTct?usp=share\\_link](https://drive.google.com/drive/folders/1DIJs3wmIpmpwI8slyHeitA6Ebe-khKTct?usp=share_link)



Figure 2: Graphical abstract of the LQIR-DG controller.

### 3. Model of the Quadrotor Platform

Here, the quadrotor platform is modeled as nonlinear. Then, a state-space model and a linear model are developed for control purposes to be utilized in the controller strategy. Finally, a nonlinear identification method is applied to identify the parameters of the quadrotor.

#### 3.1. Quadrotor Configuration

According to Figure 3, the 3-DoF quadrotor schematic is including four rotors rotating the  $z_B$  axis in the body frame with a rotational velocity,  $\Omega_i$  ( $i = 1, 2, 3, 4$ ). To eliminate the yawing moment, rotors (2, 4) and (1, 3) rotate clockwise and counter clockwise, respectively.

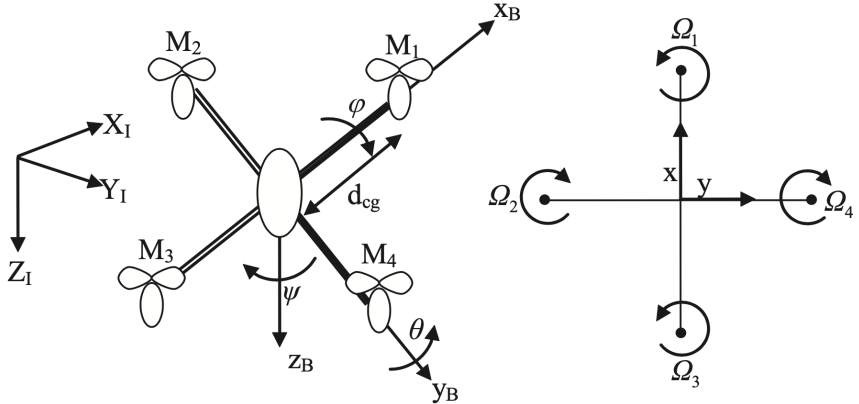


Figure 3: Quadrotor configuration.

### 3.2. Dynamic Modeling of the Quadrotor Platform

Here, according to Newton-Euler, the model of the quadrotor platform is presented as follows [7, 6]:

$$\dot{p} = \Gamma_1 pq - \Gamma_2 qr + \Gamma_3 bd_{cg}(\Omega_{c,2}^2 - \Omega_{c,4}^2) + \Gamma_4 d(\Omega_{c,1}^2 - \Omega_{c,2}^2 + \Omega_{c,3}^2 - \Omega_{c,4}^2) + \Gamma_5 \Omega_{c,r} + \Gamma_3 d_{roll} + \Gamma_4 d_{yaw} \quad (1)$$

$$\dot{q} = \Gamma_6 pr - \Gamma_7(p^2 - r^2) + \Gamma_8 bd_{cg}(\Omega_{c,1}^2 - \Omega_{c,3}^2) + \Gamma_9 \Omega_{c,r} + \Gamma_8 d_{pitch} \quad (2)$$

$$\dot{r} = \Gamma_{10} pq - \Gamma_1 qr + \Gamma_{11}(\Omega_{c,1}^2 - \Omega_{c,2}^2 + \Omega_{c,3}^2 - \Omega_{c,4}^2) + \Gamma_4 bd_{cg}(\Omega_{c,2}^2 - \Omega_{c,4}^2) + \Gamma_{11} d_{roll} + \Gamma_4 d_{yaw} \quad (3)$$

In the above equations,  $\Gamma_i$  ( $i = 1, \dots, 11$ ) is defined as

$$\begin{aligned} \Gamma_1 &= \frac{I_{xz}(I_{xx} - I_{yy} + I_{zz})}{\Gamma}, & \Gamma_2 &= \frac{I_{zz}(I_{zz} - I_{yy}) + I_{xz}^2}{\Gamma}, & \Gamma_3 &= \frac{I_{zz}}{\Gamma}, & \Gamma_4 &= \frac{I_{xz}}{\Gamma} \\ \Gamma_5 &= \frac{I_{rotor}}{I_{xx}}, & \Gamma_6 &= \frac{I_{zz} - I_{xx}}{I_{yy}}, & \Gamma_7 &= \frac{I_{xz}}{I_{yy}}, & \Gamma_8 &= \frac{1}{I_{yy}} \\ \Gamma_9 &= \frac{I_{rotor}}{I_{yy}}, & \Gamma_{10} &= \frac{(I_{xx} - I_{yy}) + I_{xz}^2}{\Gamma}, & \Gamma_{11} &= \frac{I_{xx}}{\Gamma} \end{aligned} \quad (4)$$

Moreover  $\Gamma = J_x J_z - J_{xy}^2$ . where  $\Omega_{c,i}$  ( $i = 1, 2, 3, 4$ ) is the rotational velocity, computed as

$$\Omega_{c,1}^2 = \Omega_{mean}^2 + \frac{1}{2bd_{cg}}u_{pitch} + \frac{1}{4d}u_{yaw} \quad (5)$$

$$\Omega_{c,2}^2 = \Omega_{mean}^2 + \frac{1}{2bd_{cg}}u_{roll} - \frac{1}{4d}u_{yaw} \quad (6)$$

$$\Omega_{c,3}^2 = \Omega_{mean}^2 - \frac{1}{2bd_{cg}}u_{pitch} + \frac{1}{4d}u_{yaw} \quad (7)$$

$$\Omega_{c,4}^2 = \Omega_{mean}^2 - \frac{1}{2bd_{cg}}u_{roll} - \frac{1}{4d}u_{yaw} \quad (8)$$

In the above equation,  $\Omega_{mean}$  is the rotational velocity of the rotors. Also,  $d_{cg}$ ,  $d$ , and  $b$  represent the distance between the rotors and the gravity center, drag factor, and thrust factor, respectively.  $d_{roll}$ ,  $d_{pitch}$ , and  $d_{yaw}$  denote the disturbances produced in the body coordinate frame. Additionally,  $u_{roll}$ ,  $u_{pitch}$ , and  $u_{yaw}$  are control commands generated by the LQIR-DG controller.  $I_{xx}$ ,  $I_{yy}$ , and  $I_{zz}$  are the moments of inertia. Euler angle rates are also determined from angular body rates as follows:

$$\begin{bmatrix} \dot{\phi} \\ \dot{\theta} \\ \dot{\psi} \end{bmatrix} = \begin{bmatrix} 1 & \sin(\phi)\tan(\theta) & \cos(\phi)\tan(\theta) \\ 0 & \cos(\phi) & -\sin(\phi) \\ 0 & \sin(\phi)/\cos(\theta) & \cos(\phi)/\cos(\theta) \end{bmatrix} \begin{bmatrix} p \\ q \\ r \end{bmatrix} \quad (9)$$

### 3.3. State-Space Formulation

By defining  $\mathbf{x}_{roll} = [x_1 \ x_2]^T = [p \ \phi]^T$ ,  $\mathbf{x}_{pitch} = [x_3 \ x_4]^T = [q \ \theta]^T$ , and  $\mathbf{x}_{yaw} = [x_5 \ x_6]^T = [r \ \psi]^T$ , as well as by considering the control inputs as

$$\mathbf{u} = [u_{roll} \ u_{pitch} \ u_{yaw}] = [bd_{cg}(\Omega_{c,2}^2 - \Omega_{c,4}^2) \ bd_{cg}(\Omega_{c,1}^2 - \Omega_{c,3}^2) \ bd_{cg}(\Omega_{c,1}^2 - \Omega_{c,2}^2 + \Omega_{c,3}^2 - \Omega_{c,4}^2)]$$

The nonlinear model of the quadrotor platform in the state-space form  $\dot{\mathbf{x}} = \mathbf{f}(\mathbf{x}, \mathbf{u})$  is presented as follows:

$$f_1 = \dot{x}_1 = \Gamma_1 x_1 x_3 - \Gamma_2 x_3 x_5 + \Gamma_3(u_{roll} + d_{roll}) + \Gamma_4 d(u_{yaw} + d_{yaw}) + \Gamma_5 \Omega_{c,r} \quad (10)$$

$$f_2 = \dot{x}_2 = x_1 + (x_3 \sin(x_2) + x_3 \cos(x_2)) \tan(x_4) \quad (11)$$

$$f_3 = \dot{x}_3 = \Gamma_6 x_1 x_5 - \Gamma_7(x_1^2 - x_5^2) + \Gamma_8(u_{pitch} + d_{pitch}) - \Gamma_9 \Omega_{c,r} \quad (12)$$

$$f_4 = \dot{x}_4 = x_3 \cos(x_4) - x_5 \sin(x_2) \quad (13)$$

$$f_5 = \dot{x}_5 = \Gamma_{10} x_1 x_3 - \Gamma_1 x_3 x_5 + \Gamma_{11}(u_{yaw} + d_{yaw}) + \Gamma_4(u_{roll} d_{roll}) \quad (14)$$

$$f_6 = \dot{x}_6 = \frac{x_3 \sin(x_4) + x_5 \cos(x_2)}{\cos(x_4)} \quad (15)$$

The measurement vector, obtained from the AHRS, is presented as follows:

$$\mathbf{z} = [p \ q \ r \ \phi \ \theta \ \psi]^T + \boldsymbol{\nu} \quad (16)$$

where  $\boldsymbol{\nu}$  is a Gaussian white noise. Moreover, the superscripts T indicate the transpose notation.

### 3.4. Linear Model

By defining  $\dot{\mathbf{x}} = [\dot{\mathbf{x}}_{\text{roll}} \ \dot{\mathbf{x}}_{\text{pitch}} \ \dot{\mathbf{x}}_{\text{yaw}}]^T$ , the linear model of the quadrotor platform represented about the equilibrium points ( $\mathbf{x}_e^* = 0$  and  $\mathbf{u}_e^* = 0$ ) as

$$\dot{\mathbf{x}} = \mathbf{A} \mathbf{x} + \mathbf{B} (\mathbf{u} + \mathbf{d}) \quad (17)$$

where  $\mathbf{d} = \text{diag}([d_{\text{roll}}, d_{\text{pitch}}, d_{\text{yaw}}])$  denotes the input disturbance.  $\mathbf{A}$  is the dynamic system matrix, denoted as

$$\mathbf{A} = \begin{bmatrix} \mathbf{A}_{\text{roll}} & \mathbf{0} & \mathbf{0} \\ \mathbf{0} & \mathbf{A}_{\text{pitch}} & \mathbf{0} \\ \mathbf{0} & \mathbf{0} & \mathbf{A}_{\text{yaw}} \end{bmatrix} \quad (18)$$

$\mathbf{A}_{\text{roll}} = \mathbf{A}_{\text{pitch}} = \mathbf{A}_{\text{yaw}} = \begin{bmatrix} 0 & 0 \\ 1 & 0 \end{bmatrix}$ . Also,  $\mathbf{B}$  is the input matrix defined as

$$\mathbf{B} = \begin{bmatrix} \Gamma_3 & 0 & \Gamma_4 \\ 0 & 0 & 0 \\ 0 & \Gamma_8 & 0 \\ 0 & 0 & 0 \\ \Gamma_4 & 0 & \Gamma_{11} \\ 0 & 0 & 0 \end{bmatrix} \quad (19)$$

### 3.5. Identification of the Platform Parameters

In this section, the Nonlinear Least Squares (NLS) algorithm is utilized for estimating the model parameters ( $\boldsymbol{\Gamma}$ ) of the 3-DoF experimental platform using experimental data. This technique is based on the Trust-Region Reflective (TRR) method, which finds the best values for  $\boldsymbol{\Gamma}$  by minimizing a cost function, defined as

$$\min_{\boldsymbol{\Gamma}} (\| e(\boldsymbol{\Gamma}) \|^2) = \min_{\boldsymbol{\Gamma}} \left( \sum_{j=1}^n (\mathbf{z}_j - \tilde{\mathbf{z}}_j)(\mathbf{z}_j - \tilde{\mathbf{z}}_j)^T \right) \quad (20)$$

where  $\mathbf{z}$  and  $\tilde{\mathbf{z}}$  are the experimental and simulated output signals when the same input signals are applied. Moreover,  $n$  is the number of scenarios. To find a vector  $\boldsymbol{\Gamma}$ , the optimization process performs until convergence is achieved. The structure of the identification approach is illustrated in figure 4.

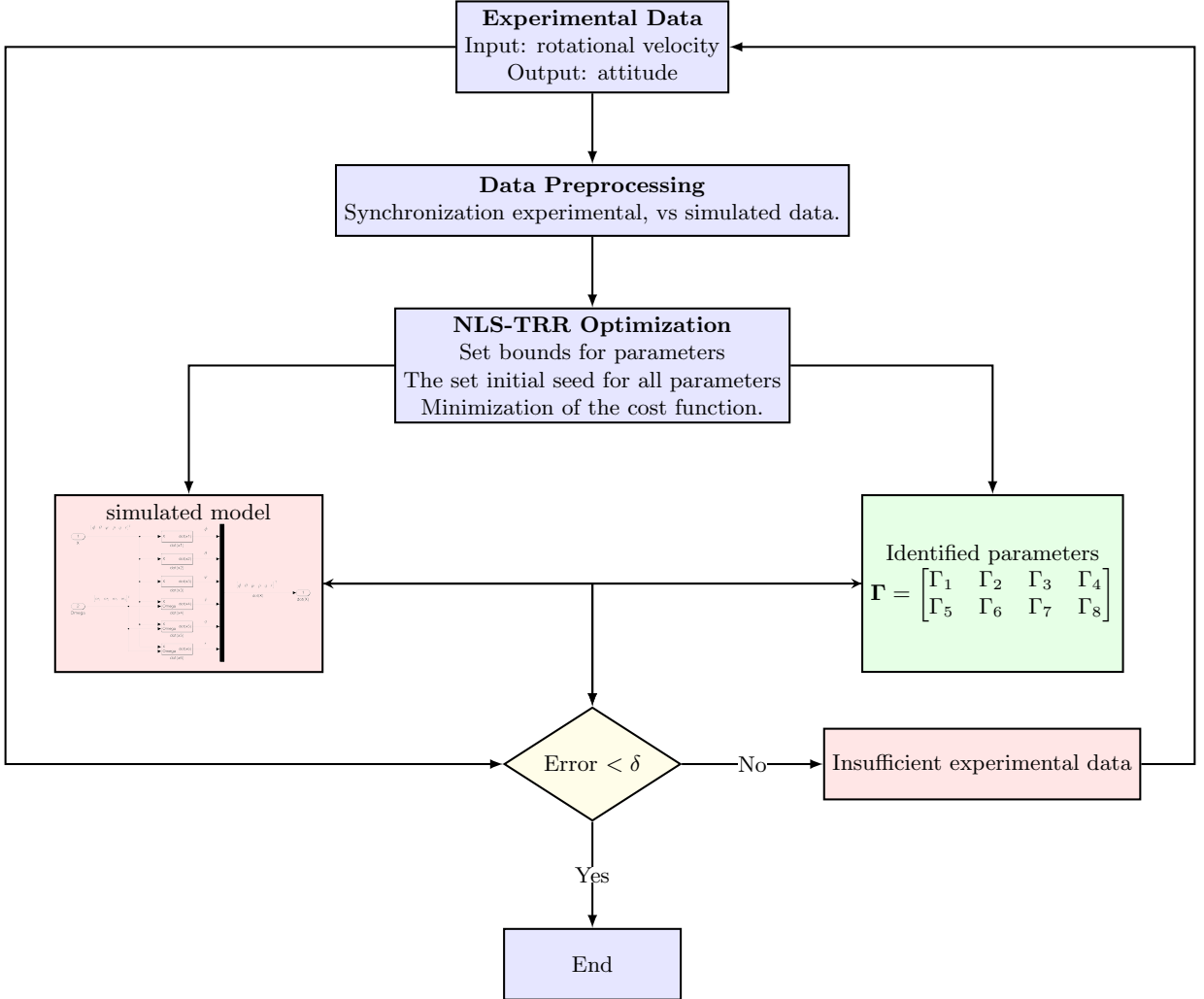


Figure 4: Structure of TRRLS identification approach.

#### 4. LQIR-DG Controller Structure

First, the augmented states of the quadrotor platform, including the states and their integrals are selected to use in the structure of the LQIR-DG controller for eliminating the steady-state errors. Then, the design methodology of the controller structure is introduced to produce the best commands for the 3-DoF quadrotor platform.

##### 4.1. Augmented States

To augment an integral action into the control strategy architecture, the augmented states are defined as  $\mathbf{x}_a = \begin{bmatrix} \mathbf{x} & \int \mathbf{x} \end{bmatrix}^T$ . Then, the quadrotor platform model, utilized in the controller structure, is presented as

$$\dot{\mathbf{x}}_a = \begin{bmatrix} \mathbf{A} & \mathbf{0} \\ \mathbf{I} & \mathbf{0} \end{bmatrix} \mathbf{x}_a + \begin{bmatrix} \mathbf{B} \\ \mathbf{0} \end{bmatrix} (\mathbf{u} + \mathbf{d}) \quad (21)$$

The notation  $\mathbf{I}$  denotes the identity matrix.

#### 4.2. LQIR-DG Control Scheme with Integral Action

In the proposed controller scheme, two fundamental players are selected in accordance with the game theory approach. The primary player determines the control commands, while another player generates the worst possible disturbance. To achieve the primary objective, the first player minimizes the following cost function but the other player maximizes it:

$$\min_u \max_d J(\mathbf{x}_{\mathbf{a}_i}, d_i, u_i) = \min_d \max_u \int_0^{t_f} \left( \mathbf{x}_{\mathbf{a}_i}^T \mathbf{Q}_i \mathbf{x}_{\mathbf{a}_i} + u_i^T R u_i - d_i^T R_d d_i \right) dt \quad (22)$$

where  $t_f$  is the stop time and  $i$ -index denotes the roll, pitch, and yaw channels of the quadrotor.  $\mathbf{Q}_i$ ,  $R_d$ , and  $R$  are weight coefficients of the cost function. By solving the above problem, the optimal control command is computed as follows [11]:

$$u_i = -\mathbf{K}_i \mathbf{x}_{\mathbf{a}_i} \quad (23)$$

Moreover, the worst disturbance is obtained as

$$d_i = \mathbf{K}_{\mathbf{d}_i} \mathbf{x}_{\mathbf{a}_i} \quad (24)$$

Here,  $\mathbf{K}_{\mathbf{d}_i}$  and  $\mathbf{K}_i$  are gain values defined as follows:

$$\mathbf{K}_{\mathbf{d}_i} = R_d^{-1} \mathbf{B}_{a_{d_i}}^T \mathbf{P}_{a_{d_i}} \quad (25)$$

$$\mathbf{K}_i = R^{-1} \mathbf{B}_{a_i}^T \mathbf{P}_{a_i} \quad (26)$$

$\mathbf{P}_{a_i}$  and  $\mathbf{P}_{a_{d_i}}$  satisfy

$$-\mathbf{A}_a^T \mathbf{P}_{a_{d_i}} - \mathbf{Q}_i - \mathbf{P}_{a_{d_i}} \mathbf{A}_a + \mathbf{P}_{a_{d_i}} \mathbf{S}_{a_i} \mathbf{P}_{a_i} + \mathbf{P}_{a_{d_i}} \mathbf{S}_{a_{d_i}} \mathbf{P}_{a_{d_i}} = \mathbf{0} \quad (27)$$

$$-\mathbf{A}_a^T \mathbf{P}_{a_i} - \mathbf{Q}_i - \mathbf{P}_{a_i} \mathbf{A}_a + \mathbf{P}_{a_i} \mathbf{S}_{a_{d_i}} \mathbf{P}_{a_{d_i}} + \mathbf{P}_{a_i} \mathbf{S}_{a_i} \mathbf{P}_{a_i} = \mathbf{0} \quad (28)$$

where  $\mathbf{S}_{a_i} = \mathbf{B}_{a_i} R^{-1} \mathbf{B}_{a_i}^T$  and  $\mathbf{S}_{a_{d_i}} = \mathbf{B}_{a_{d_i}} R_d^{-1} \mathbf{B}_{a_{d_i}}^T$ .

#### 4.3. TCACS Optimization for Tuning the Weighting Matrices

To optimize the weighting matrix of the LQIR-DG (Linear Quadratic Integral Regulator with Disturbance Rejection) controller, the TCACS (Tabu Continuous Ant Colony System) [20] optimization method was utilized. The objective was to tune the controller parameters for improved performance in a 3-degree-of-freedom simulation.

In the optimization process, the cost function was formulated based on the LQIR-DG controller, where the state feedback matrix  $\mathbf{Q}$  and the disturbance rejection matrix  $R_d$  were the key parameters to be determined. To simplify the problem, it was assumed that  $R$  (the penalty matrix for control inputs) was fixed at a value of 1.

By employing the TCACS optimization method, the algorithm explored the search space to find the optimal values of  $\mathbf{Q}$  and  $R_d$  for each channel. The objective was to achieve a balance between control effort and disturbance rejection while ensuring stable and robust control performance.

The optimization process aimed to fine-tune the controller parameters for the specific dynamics of the system under consideration. The resulting weighting matrices  $\mathbf{Q}$  and  $R_d$  would enable the LQIR-DG controller to efficiently regulate the system while effectively rejecting disturbances in the simulation. In this section, the TCACS optimization method is utilized to tune the weighting matrices of the LQIR-DG controller.

## 5. Results

The results of the parameter identification and the LQIR-DG Controller for the quadrotor platform are presented. First, the quadrotor parameters are estimated based on the NLS method. Then, the performance of the LQIR-DG structure is evaluated. Table 6 present the quadrotor and LQIR-DG parameters, respectively.

Table 1: Quadrotor parameters

| Parameter              | Unit                                   | Value                 | Parameter          | Unit              | Value                   |
|------------------------|--|-----------------------|--------------------|-------------------|-------------------------|
| $m_{\text{total}}$     | kg                                     | 1.074                 | $I_{xx}$           | kg.m <sup>2</sup> | 0.02839                 |
| d                      | N.m.sec <sup>2</sup> /rad <sup>2</sup> | $3.2 \times 10^{-6}$  | $I_{yy}$           | kg.m <sup>2</sup> | 0.03066                 |
| b                      | N.sec <sup>2</sup> /rad <sup>2</sup>   | $3.13 \times 10^{-5}$ | $I_{zz}$           | kg.m <sup>2</sup> | 0.0439                  |
| $d_{cg}$               | m                                      | 0.2                   | $I_{\text{rotor}}$ | kg.m <sup>2</sup> | $4.4398 \times 10^{-5}$ |
| $\Omega_{\text{mean}}$ | rpm                                    | 2000                  | $I_{xz}$           | kg.m <sup>2</sup> | $6.87 \times 10^{-7}$   |

Table 2: Quadrotor parameters

| Description      | Parameter              | Unit                                   | Value                 | Parameter          | Unit              | Value                   |
|------------------|------------------------|--|-----------------------|--------------------|-------------------|-------------------------|
| Mass             | $m_{\text{total}}$     | kg                                     | 1.074                 | $I_{xx}$           | kg.m <sup>2</sup> | 0.02839                 |
| Inertia          | d                      | N.m.sec <sup>2</sup> /rad <sup>2</sup> | $3.2 \times 10^{-6}$  | $I_{yy}$           | kg.m <sup>2</sup> | 0.03066                 |
| Drag             | b                      | N.sec <sup>2</sup> /rad <sup>2</sup>   | $3.13 \times 10^{-5}$ | $I_{zz}$           | kg.m <sup>2</sup> | 0.0439                  |
| CG Distance      | $d_{cg}$               | m                                      | 0.2                   | $I_{\text{rotor}}$ | kg.m <sup>2</sup> | $4.4398 \times 10^{-5}$ |
| Mean Rotor Speed | $\Omega_{\text{mean}}$ | rpm                                    | 2000                  | $I_{xz}$           | kg.m <sup>2</sup> | $6.87 \times 10^{-7}$   |

Table 3: Quadrotor parameters

| Parameter              | Unit                                   | Value                   | Description           |
|------------------------|--|-------------------------|-----------------------|
| $m_{\text{total}}$     | kg                                     | 1.074                   | Total Mass            |
| d                      | N.m.sec <sup>2</sup> /rad <sup>2</sup> | $3.2 \times 10^{-6}$    | Drag Factor           |
| b                      | N.sec <sup>2</sup> /rad <sup>2</sup>   | $3.13 \times 10^{-5}$   | Thrust Factor         |
| $d_{cg}$               | m                                      | 0.2                     | CG Distance           |
| $\Omega_{\text{mean}}$ | rpm                                    | 2000                    | Mean Rotor Speed      |
| $I_{xx}$               | kg.m <sup>2</sup>                      | 0.02839                 | Inertia about X-axis  |
| $I_{yy}$               | kg.m <sup>2</sup>                      | 0.03066                 | Inertia about Y-axis  |
| $I_{zz}$               | kg.m <sup>2</sup>                      | 0.0439                  | Inertia about Z-axis  |
| $I_{\text{rotor}}$     | kg.m <sup>2</sup>                      | $4.4398 \times 10^{-5}$ | Rotor Inertia         |
| $I_{xz}$               | kg.m <sup>2</sup>                      | $6.87 \times 10^{-7}$   | Inertia about XZ-axis |

Table 4: Quadrotor parameters

| Shape            | Parameter              | Unit                                   | Value                 | Description                     |
|------------------|------------------------|--|-----------------------|---------------------------------|
| Mass             | $m_{\text{total}}$     | kg                                     | 1.074                 | Total mass of the quadrotor     |
| Inertia          | $d$                    | N.m.sec <sup>2</sup> /rad <sup>2</sup> | $3.2 \times 10^{-6}$  | Moment of inertia about xx-axis |
| Inertia          | $I_{yy}$               | kg.m <sup>2</sup>                      | 0.03066               | Moment of inertia about yy-axis |
| Drag             | $b$                    | N.sec <sup>2</sup> /rad <sup>2</sup>   | $3.13 \times 10^{-5}$ | Drag coefficient                |
| CG Distance      | $d_{cg}$               | m                                      | 0.2                   | Center of gravity distance      |
| Mean Rotor Speed | $\Omega_{\text{mean}}$ | rpm                                    | 2000                  | Mean rotor speed                |

Table 5: Quadrotor parameters

| Parameter              | Unit                                   | Value                 | Description      | Parameter          | Unit              | Value                   | Description           |
|------------------------|--|-----------------------|------------------|--------------------|-------------------|-------------------------|-----------------------|
| $m_{\text{total}}$     | kg                                     | 1.074                 | Mass             | $I_{xx}$           | kg.m <sup>2</sup> | 0.02839                 | Inertia X-axis        |
| $d$                    | N.m.sec <sup>2</sup> /rad <sup>2</sup> | $3.2 \times 10^{-6}$  | Drag Factor      | $I_{yy}$           | kg.m <sup>2</sup> | 0.03066                 | Inertia Y-axis        |
| $b$                    | N.sec <sup>2</sup> /rad <sup>2</sup>   | $3.13 \times 10^{-5}$ | Thrust Factor    | $I_{zz}$           | kg.m <sup>2</sup> | 0.0439                  | Inertia Z-axis        |
| $d_{cg}$               | m                                      | 0.2                   | CG Distance      | $I_{\text{rotor}}$ | kg.m <sup>2</sup> | $4.4398 \times 10^{-5}$ | Rotor Inertia         |
| $\Omega_{\text{mean}}$ | rpm                                    | 2000                  | Mean Rotor Speed | $I_{xz}$           | kg.m <sup>2</sup> | $6.87 \times 10^{-7}$   | Inertia about XZ-axis |

Table 6: Quadrotor parameters

| Parameter              | Unit                                   | Value                   | Description           |
|------------------------|--|-------------------------|-----------------------|
| $m_{\text{total}}$     | kg                                     | 1.074                   | Mass                  |
| $d$                    | N.m.sec <sup>2</sup> /rad <sup>2</sup> | $3.2 \times 10^{-6}$    | Drag Factor           |
| $b$                    | N.sec <sup>2</sup> /rad <sup>2</sup>   | $3.13 \times 10^{-5}$   | Thrust Factor         |
| $d_{cg}$               | m                                      | 0.2                     | CG Distance           |
| $\Omega_{\text{mean}}$ | rpm                                    | 2000                    | Mean Rotor Speed      |
| $I_{xx}$               | kg.m <sup>2</sup>                      | 0.02839                 | Inertia X-axis        |
| $I_{yy}$               | kg.m <sup>2</sup>                      | 0.03066                 | Inertia Y-axis        |
| $I_{zz}$               | kg.m <sup>2</sup>                      | 0.0439                  | Inertia Z-axis        |
| $I_{\text{rotor}}$     | kg.m <sup>2</sup>                      | $4.4398 \times 10^{-5}$ | Rotor Inertia         |
| $I_{xz}$               | kg.m <sup>2</sup>                      | $6.87 \times 10^{-7}$   | Inertia about XZ-axis |

### 5.1. Challenges in Designing and Implementation

Developing and implementing advanced control strategies for unmanned aerial vehicles (UAVs) presents several challenges that need careful consideration to ensure successful deployment in real-world scenarios. In this subsection, we briefly highlight the key challenges encountered during the design and implementation of the proposed controller.

1. **Nonlinear Dynamics:** quadrotors exhibit highly nonlinear and coupled dynamics, which demand sophisticated control algorithms to achieve precise and stable control.

2. **Model Uncertainty:** Accurate modeling of quadrotor dynamics is challenging due to uncertainties in aerodynamics, payload, and external disturbances. Robust control techniques are required to address model uncertainties effectively.
3. **Sensor Noise and Calibration:** Real-world sensors are prone to noise and calibration errors, affecting state estimation accuracy. Sensor fusion and calibration techniques are essential for reliable control.
4. **Real-time Computation:** quadrotor control systems must execute in real-time, necessitating computationally efficient algorithms to ensure low-latency response.
5. **Robustness to External Disturbances:** quadrotors operate in dynamic and unpredictable environments, making them susceptible to wind gusts and other disturbances. Robust control strategies are essential to maintain stability.
6. **Safety and Collision Avoidance:** Ensuring safety during quadrotor operation is critical, requiring collision avoidance algorithms and fail-safe mechanisms.
7. **Experimental Validation:** Real-world testing and validation of the controller pose logistical and safety challenges, requiring careful experimental setups.

Addressing these challenges is crucial to ensure the successful deployment and practicality of the proposed controller in real-world applications.

### 5.2. Tuning of LQIR-DG Weighting Matrices

The TCACS (Tabu Continuous Ant Colony System) optimization method was employed to fine-tune the LQIR-DG weighting matrices  $\mathbf{Q}$  and  $R_d$  of the LQIR-DG controller. Due to the relation between the weighting matrices is important, the  $R$  matrix is assumed as 1, while the weighting matrix  $\mathbf{Q}$  is represented as  $\text{diag}([\mathbf{Q}_{\text{roll}}, \mathbf{Q}_{\text{pitch}}, \mathbf{Q}_{\text{yaw}}])$ , and  $R_d$  is individually optimized for each channel. The primary objective was to enhance the controller's performance in a 3-degree-of-freedom simulation by minimizing the ITSE cost function, thereby ensuring stable and robust control performance while addressing control effort and disturbance rejection. The pseudo code of TCACS is shown in Algorithm 1.

The parameters of the LQIR-DG controller approach, including weight coefficients ( $\mathbf{Q}_i$  for  $i = \text{roll}, \text{pitch}, \text{yaw}$ ,  $R_d$ , and  $R$ ) are tuned using a heuristic optimization algorithm based on the Tabu Continuous Ant Colony System (TCACS) [15] approach. In this method, ants utilize the concepts of promising list and tabu balls to move toward the goal ant gradually. The pseudo-code of TCACS is shown in Figure 5. For this purpose, ants find the promising areas to contain the global minimum and perform searching within tabu balls of the bad regions. TCACS parameters are shown in Table 7. Here, it is assumed that the value of  $R$  is identical for all attitude channels and considered with the value of 1. Moreover, the initial values of the ants position ( $\mathbf{Q}_{\text{roll}}, \mathbf{Q}_{\text{pitch}}, \mathbf{Q}_{\text{yaw}}$  and  $R_d$ ) for  $l = 1, \dots, N$  is selected using a random distribution. The cost is denoted in iteration  $i$  using the quality of the tracking error between the set-point,  $\mathbf{x}_{sp}$ , and the quadrotor states,  $\mathbf{x} = [\mathbf{x}_{\text{roll}} \quad \mathbf{x}_{\text{pitch}} \quad \mathbf{x}_{\text{yaw}}]^T$  as

$$\text{ITSE} = \int_0^{t_f} t (\mathbf{x}_{sp} - \mathbf{x})^T (\mathbf{x}_{sp} - \mathbf{x}) dt \quad (29)$$

where  $t$  and  $t_f$  are the response time of the system and the final time, respectively. Finally, when the stopping condition of the TCACS algorithm is reached, the best values of the LQIR-DG parameters are computed, shown in Table 8

---

**Algorithm 1** Tabu Continuous Ant Colony System (TCACS)

---

```

1: procedure TCACS
2:   Initialize parameters, lists, and values
3:   while not terminated do
4:     if first iteration then
5:       Sample initial ant positions
6:     else
7:       Move ants
8:     end if
9:     Update structures and distributions
10:   end while
11: end procedure

```

---

Figure 5: Pseudo-code of the TCACS optimization algorithm [15].

Table 7: Parameters of the TCACS optimization algorithm.

| Parameter  | Value     | Description            |
|------------|-----------|------------------------|
| N          | 15        | Number of Ants         |
| $I_{\max}$ | 10000     | Maximum of Iteration   |
| Tolerance  | $10^{-4}$ | Maximum accepted error |

Table 8: LQIR-DG controller parameters

| Channel | Weighting Matrix            | Values  |
|---------|-----------------------------|---|
| Roll    | $\mathbf{Q}_{\text{roll}}$  | $\text{diag}([0.02, 65.96, 83.04, 0.00])$         |
| Pitch   | $\mathbf{Q}_{\text{pitch}}$ | $\text{diag}([435.01, 262.60, 262.60, 0.00])$     |
| Yaw     | $\mathbf{Q}_{\text{yaw}}$   | $\text{diag}([4 \times 10^{-4}, 0.00, 0.133, 0])$ |
| -       | $R_d$                       | 1.2764  |

### 5.3. Identification of the 3-DoF quadrotor platform model

As described in section 3.3, the parameters of the quadrotor platform, denoted by  $\Gamma_i (i = 1, \dots, 11)$ , are identified using the NLS-TRR algorithm. To increase the accuracy of parameter identification, three scenarios are considered according to Table 9. In the first scenario, depicted in Figure 6, the quadrotor rotates about only one axis (roll, pitch, or yaw axes) to identify the parameters  $\Gamma_3$ ,  $\Gamma_5$ ,  $\Gamma_8$ ,  $\Gamma_9$ , and  $\Gamma_{11}$ . In the second scenario, according to Figure 7, the parameters  $\Gamma_1$  and  $\Gamma_7$  are estimated by rotating the experimental platform around its roll and pitch axes simultaneously. Finally, Figure 8 displays the results of the third scenario including the estimation of the parameters  $\Gamma_2$ ,  $\Gamma_4$ ,  $\Gamma_6$ , and  $\Gamma_{10}$  for the UAV model, when the platform freely rotates around three axes. After the termination condition is met, the optimal values of the quadrotor parameters are computed and denoted in Table 11. These results illustrate that the outputs of the simulation results for the quadrotor model are consistent with reality.

Table 9: Scenarios for identification of quadrotor parameters.

| Scenario | Description             | Initial Condition (deg) |            |          | Rotational Velocity Commands (rpm) |            |            |            |
|----------|-------------------------|-------------------------|------------|----------|------------------------------------|------------|------------|------------|
|          |                         | $\phi_0$                | $\theta_0$ | $\psi_0$ | $\Omega_1$                         | $\Omega_2$ | $\Omega_3$ | $\Omega_4$ |
| I        | roll free               | 38                      | -          | -        | 2000                               | 2000       | 2000       | 3400       |
|          | pitch free              | -                       | -15        | -        | 3700                               | 2000       | 2000       | 2000       |
|          | yaw free                | -                       | -          | -75      | 2000                               | 3300       | 2000       | 3300       |
| II       | roll & pitch free       | 8                       | -5         | -        | 1700                               | 3800       | 2400       | 1700       |
| III      | roll, pitch, & yaw free | 8                       | -3         | -146     | 1700                               | 3800       | 2400       | 1700       |

Table 10: True values of the quadrotor parameters.

| Parameter     | Value                   | Parameter     | Value                    |
|---------------|-------------------------|---------------|--------------------------|
| $\Gamma_1$    | $4.9895 \times 10^{-6}$ | $\Gamma_6$    | 2.5294                   |
| $\Gamma_2$    | 0.0029                  | $\Gamma_7$    | 0.0002                   |
| $\Gamma_3$    | 42.1805                 | $\Gamma_8$    | 18.46                    |
| $\Gamma_4$    | 0.0002                  | $\Gamma_9$    | 0.0022                   |
| $\Gamma_5$    | -0.0023                 | $\Gamma_{10}$ | $-1.4456 \times 10^{-5}$ |
| $\Gamma_{11}$ | 24.4570                 |               |                          |

Table 11: True values of the quadrotor parameters.

| Parameter 1   | Value 1                  | Parameter 2   | Value 2 | Parameter 3 | Value 3 |
|---------------|--------------------------|---------------|---------|-------------|---------|
| $\Gamma_1$    | $4.9895 \times 10^{-6}$  | $\Gamma_2$    | 0.0029  | $\Gamma_3$  | 42.1805 |
| $\Gamma_4$    | 0.0002                   | $\Gamma_5$    | -0.0023 | $\Gamma_6$  | 2.5294  |
| $\Gamma_7$    | 0.0002                   | $\Gamma_8$    | 18.46   | $\Gamma_9$  | 0.0022  |
| $\Gamma_{10}$ | $-1.4456 \times 10^{-5}$ | $\Gamma_{11}$ | 24.4570 |             |         |

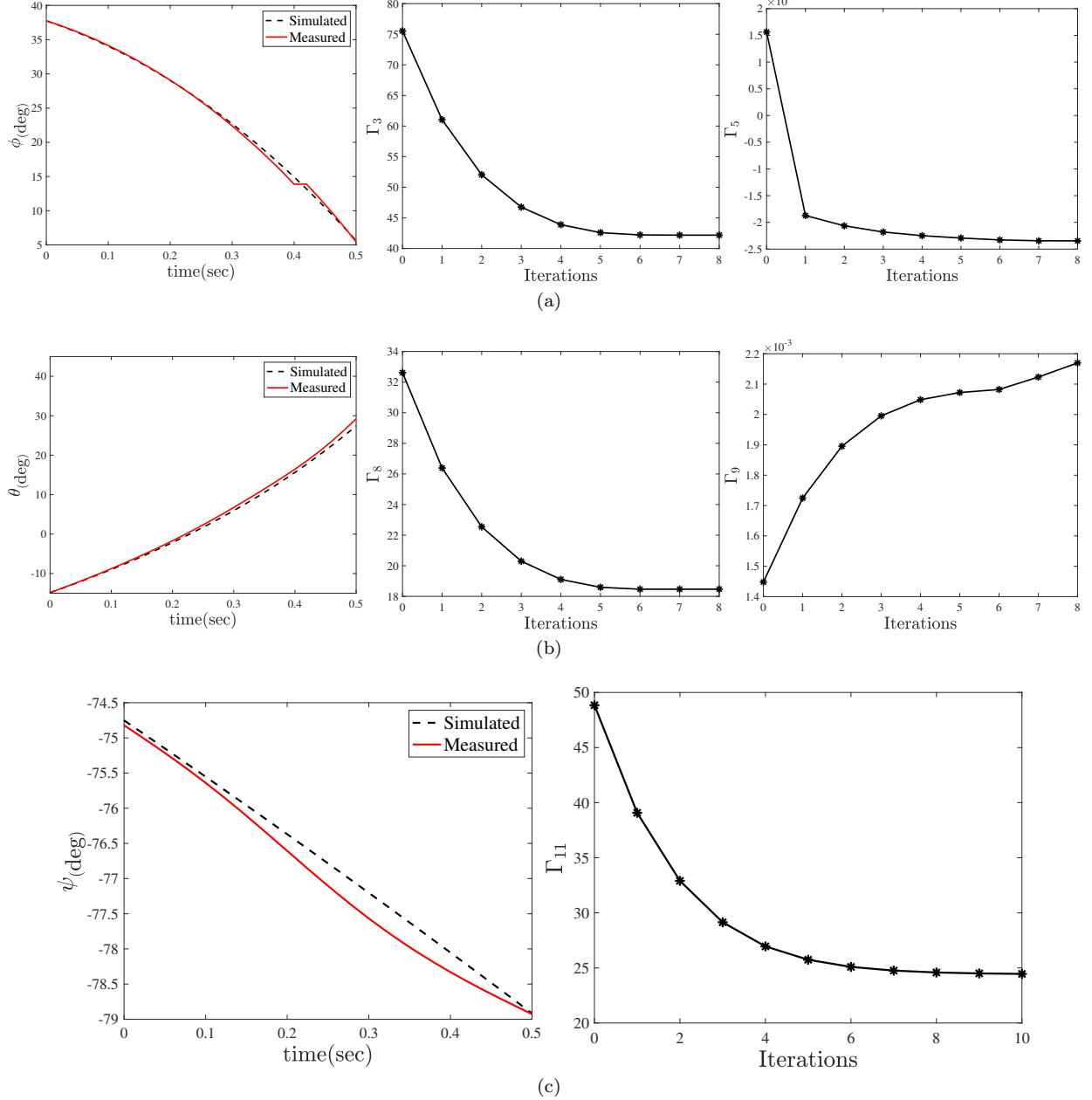
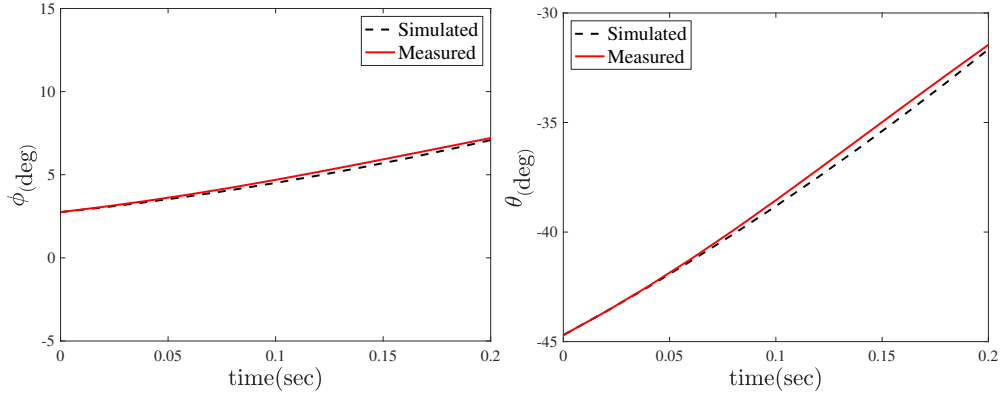
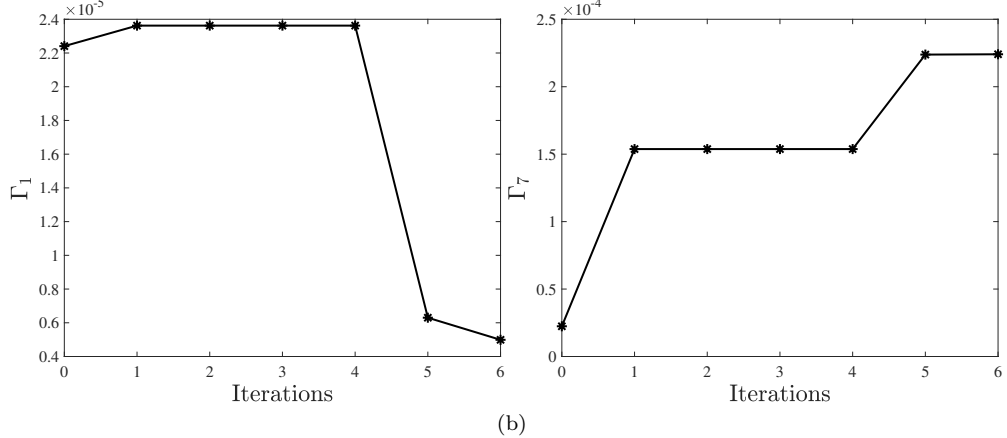


Figure 6: Identification process results when the quadrotor rotates about only one axis: (a) identification of  $\Gamma_3$  and  $\Gamma_5$  in free roll motion. (b) identification of  $\Gamma_6$  and  $\Gamma_9$  in free pitch motion. (c) identification of  $\Gamma_{11}$  in free yaw motion.

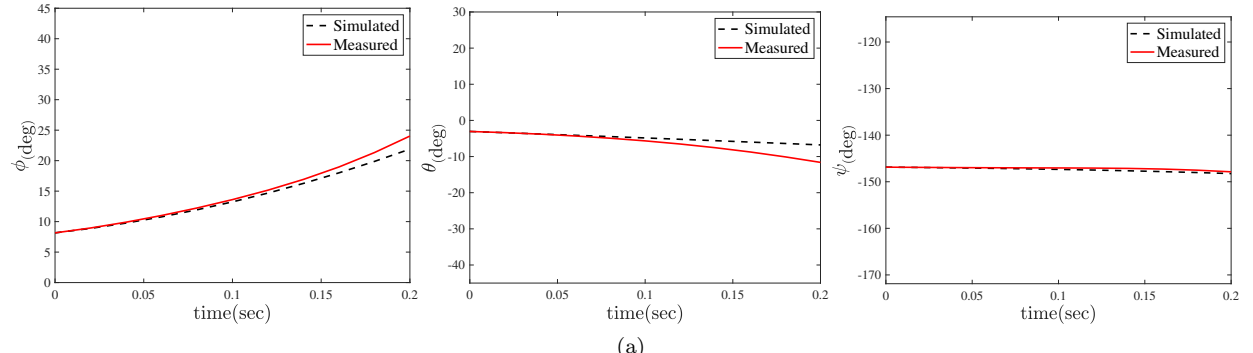


(a)

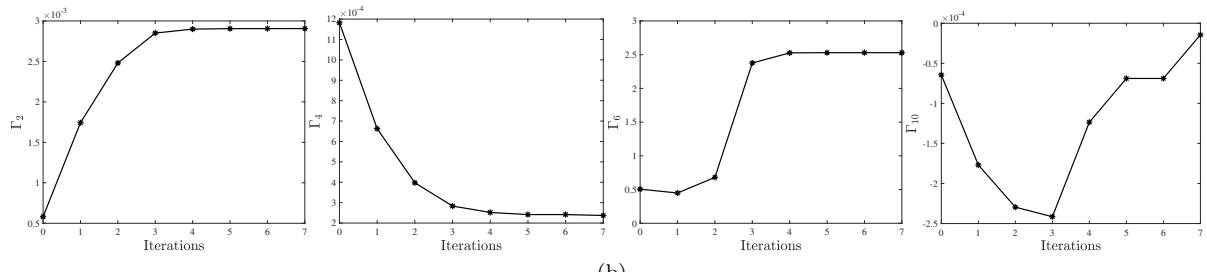


(b)

Figure 7: Identification process results when the quadrotor rotates about its roll and pitch axes: (a) comparison of simulation and experimental results. (b) identification of  $\Gamma_1$  and  $\Gamma_7$ .



(a)



(b)

Figure 8: Identification process results when the quadrotor rotates about its roll, pitch, and yaw axes: (a) comparison of simulation and experimental results. (b) identification of  $\Gamma_2$ ,  $\Gamma_4$ ,  $\Gamma_6$ , and  $\Gamma_{10}$  parameters.

#### 5.4. Evaluation of LQIR-DG Performance

In this section, the LQIR-DG controller algorithm is evaluated in three scenarios i) regulation and tracking problems, ii) disturbance rejection, and iii) impact of model uncertainty. Finally, a comparison of the proposed controller is performed with a PID controller and variants of the LQR controller. The PID controller parameters are presented in Table 12.

Table 12: PID controller parameters

| Channel | $K_p$ | $K_i$ | $K_d$ |
|---------|-------|-------|-------|
| roll    | 18    | 6     | 9     |
| pitch   | 22    | 15    | 16    |

##### 5.4.1. Investigating of the Regulation and Tracking Problems

The results of the proposed approach are presented for tracking the desired roll and pitch angles in Figures 9 and 10. Figure 9 (a) compares the desired and output signals, i.e., the Euler angles during the regulation problem. Moreover, Figure 9 (b) compares the desired square wave signals with a frequency of 0.02 Hz and an amplitude of 20 degrees with the output signals, when the quadrotor platform freely rotates around roll and pitch simultaneously. Figures 10 (a) and (b) show the rotational velocity commands of the quadrotor in the regulation and tracking problems, respectively. These results demonstrate that the roll and pitch angles are accurately controlled by the proposed approach.

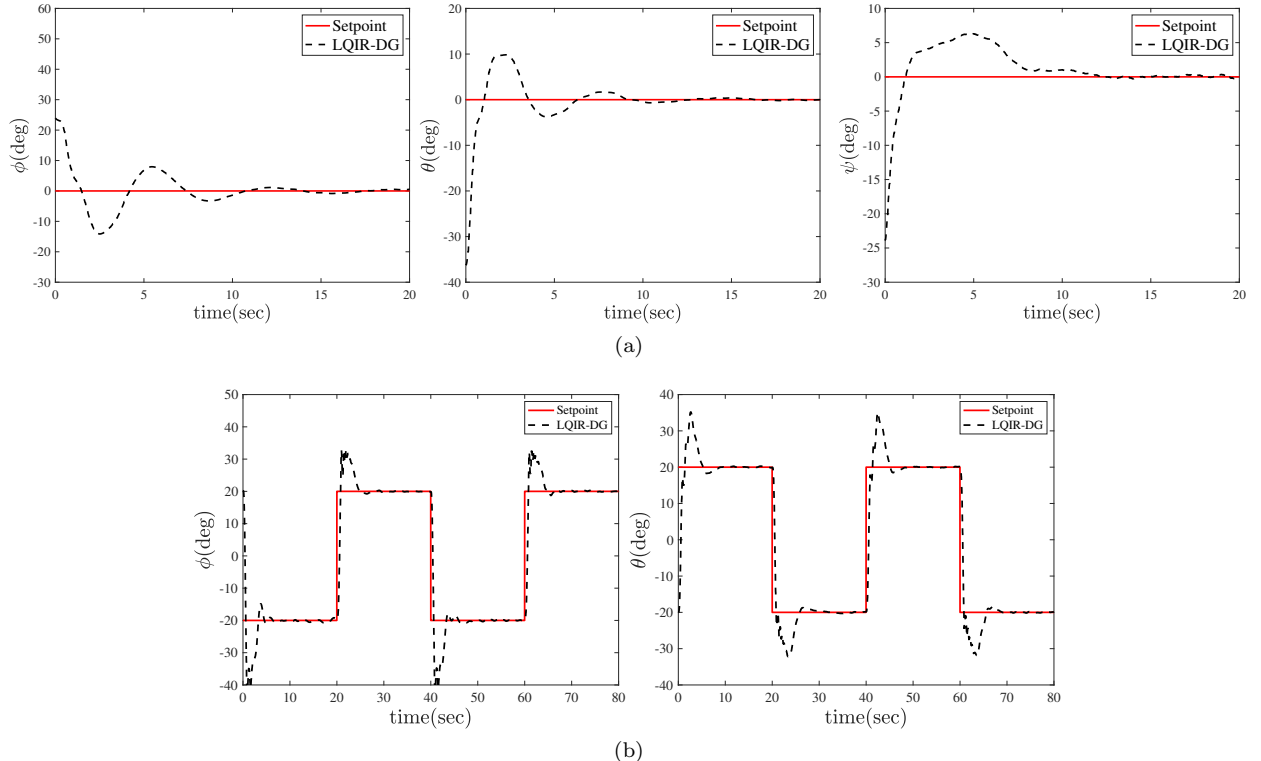


Figure 9: Comparison of actual roll and pitch angles with the desired values in (a) regulation and (b) tracking problems.

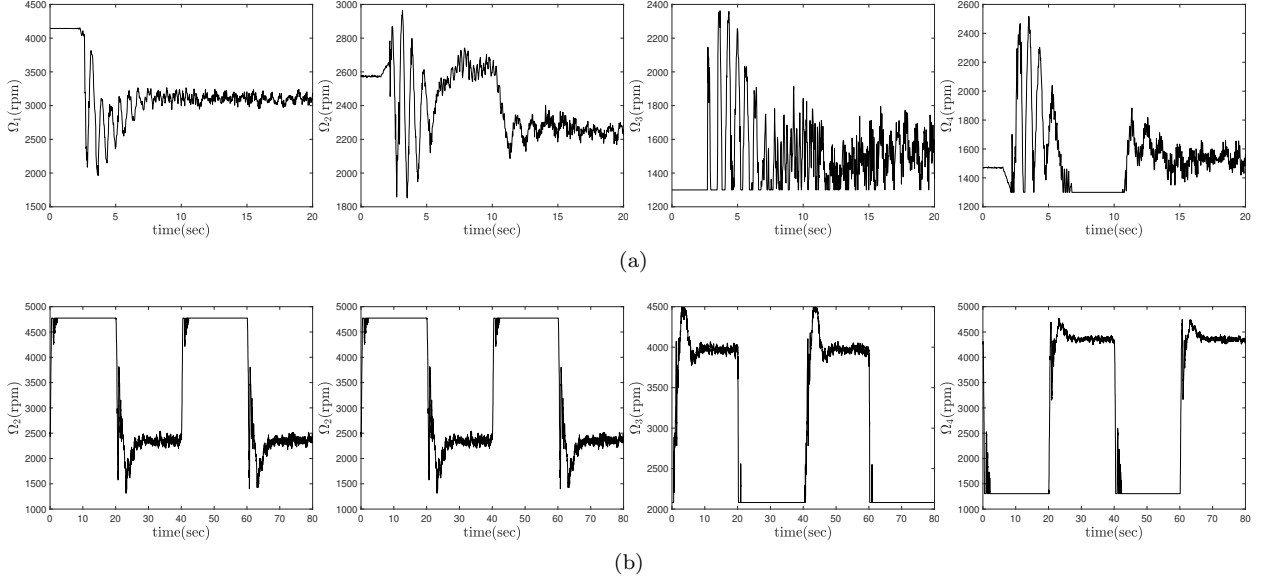


Figure 10: Rotational velocity commands in (a) regulation and (b) tracking problems.

#### 5.4.2. Investigating the Disturbance Rejection

Here, the effect of the input disturbance is investigated on the performance of the proposed controller. The input disturbance,  $d_{\Omega_i}$ , is considered as a change in command of the rotational velocity, modeled as

$$d_{\Omega_1} = d_{\Omega_2} = -d_{\Omega_3} = -d_{\Omega_4} = \begin{cases} 500 \text{ rpm} & 20 < t < 60 \\ 0 & \text{otherwise} \end{cases} \quad (30)$$

Figure 11 illustrates the roll and pitch angles in the regulation problem when the input disturbance occurs. These results indicate that the proposed controller can stabilize the quadrotor platform in the presence of input disturbance.

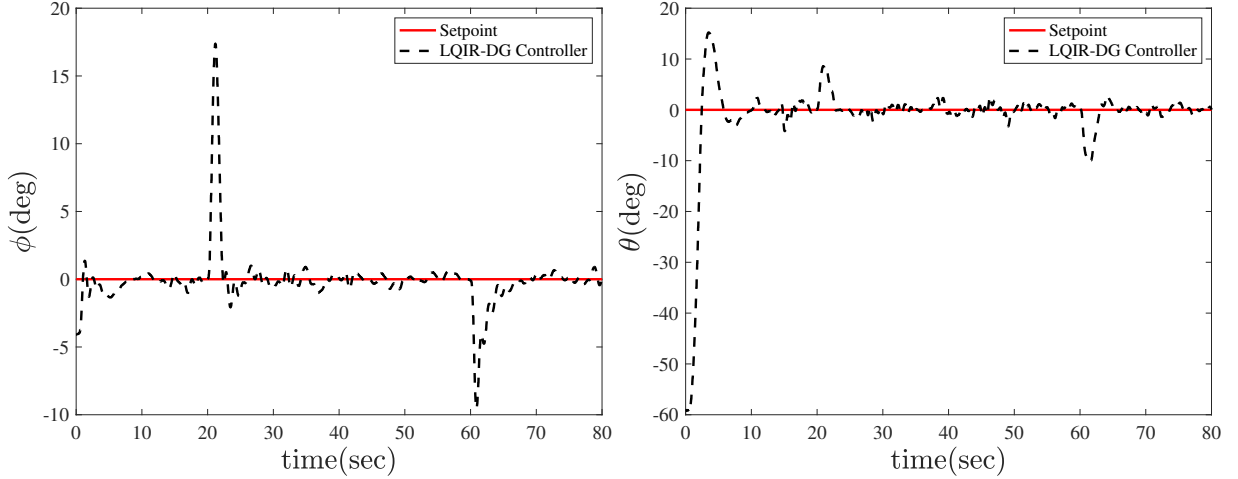


Figure 11: Comparison of actual roll and pitch angles with the desired, when the input disturbance occurs.

#### 5.4.3. Investigating the Impact of Modeling Uncertainty

The effect of the modeling uncertainty is investigated on the performance of the proposed controller. To achieve this, 50 and 100 grams weights are added to the roll and pitch axes, respectively, as shown in Figure 12. Figure 13 (a) compares the desired and the actual roll angle and Figure 13 (b) shows the desired and the actual pitch angle, when the uncertainty of moments of inertia is present. Moreover, Figure 13 (c) shows the rotational velocity commands of the experimental platform, when the model uncertainty is applied. The implementation results show that the platform outputs converge to the desired values in the presence of the modeling uncertainty.

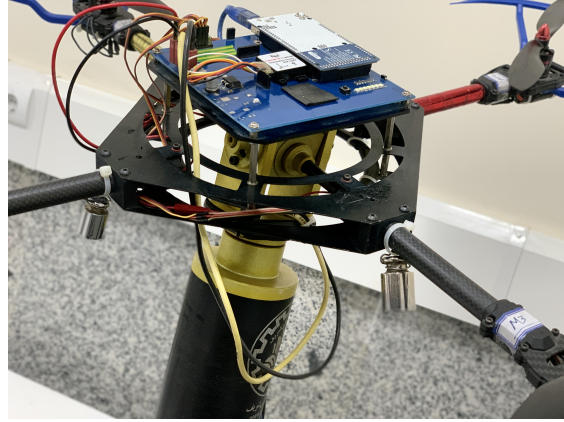


Figure 12: Quadrotor 3-DoF platform with added weights.

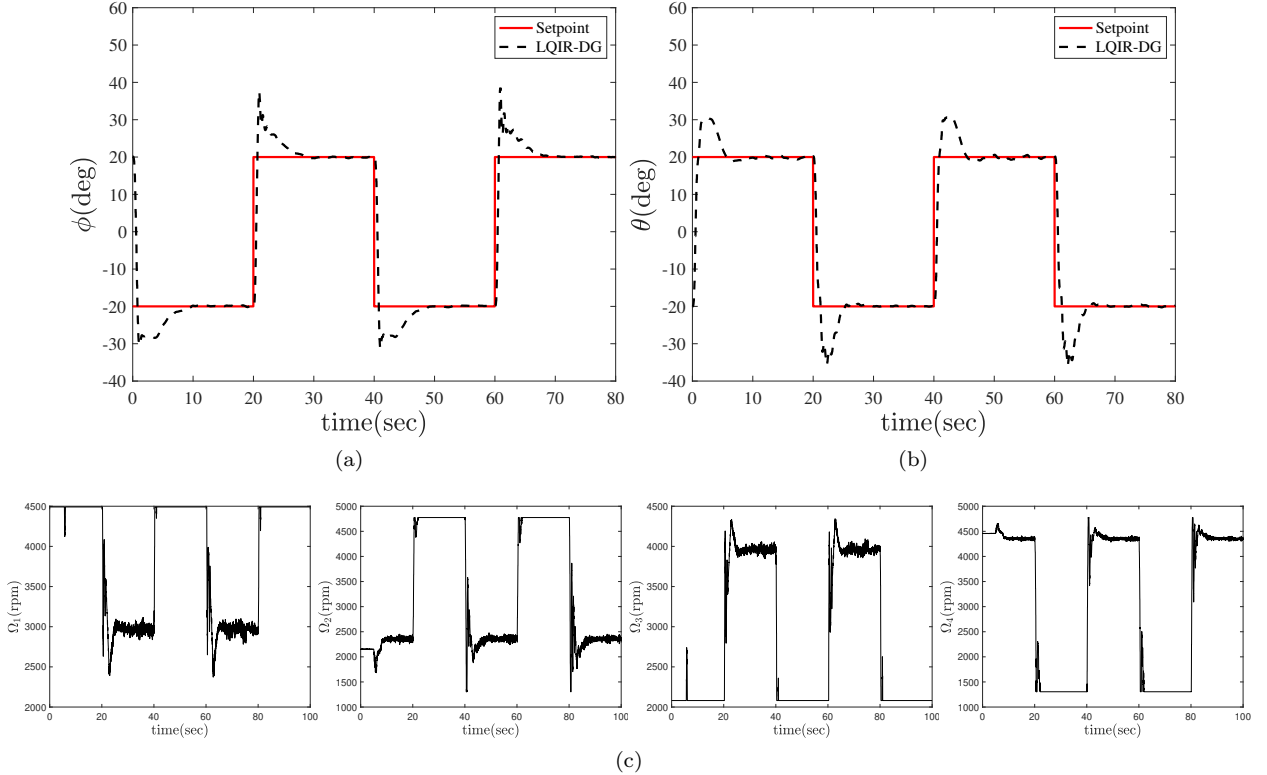


Figure 13: Comparison of actual roll and pitch angles with desired values, when the modeling uncertainty is present.

#### 5.4.4. Comparison with the Control Strategies

Figure 16 compares the LQIR-DG controller performance with the PID controller and variant of the LQR strategies such as the LQR and LQIR. Moreover, the box plot of all controllers is plotted in Figure 15 for the cost function, introduced in equation (22). The median of Root Mean Square Error (RMSE) is shown in the crossline in the box plot. These results indicate that the proposed controller is able to provide rapid convergence and excellent transient response relative to other controllers for attitude control of the experimental platform.

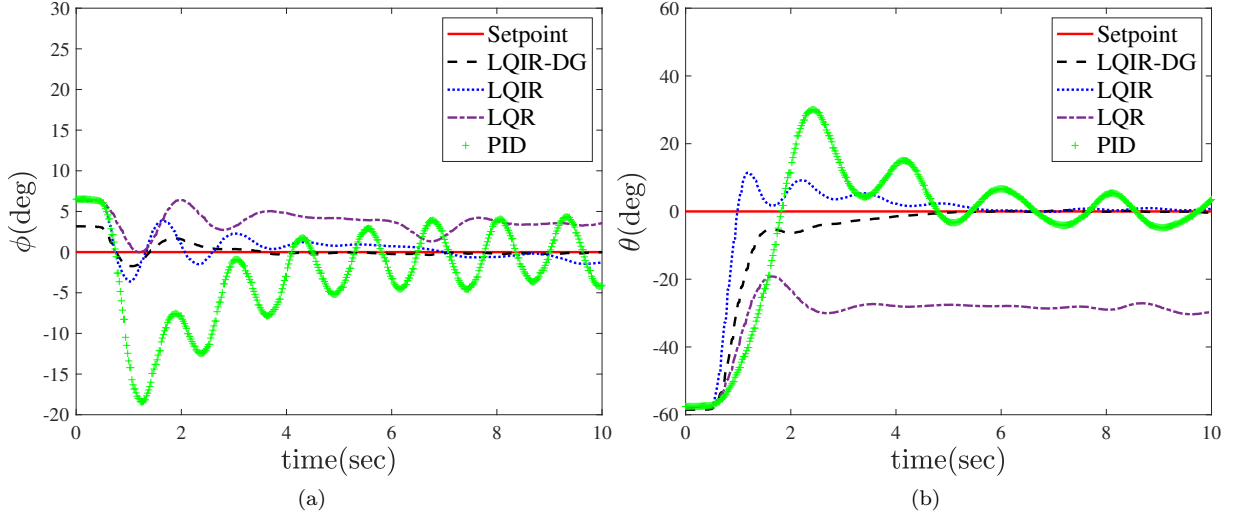


Figure 14: Comparison of LQIR-DG structure with the variant of LQR and PID in regulation problem: (a) roll angle (d) pitch angle.

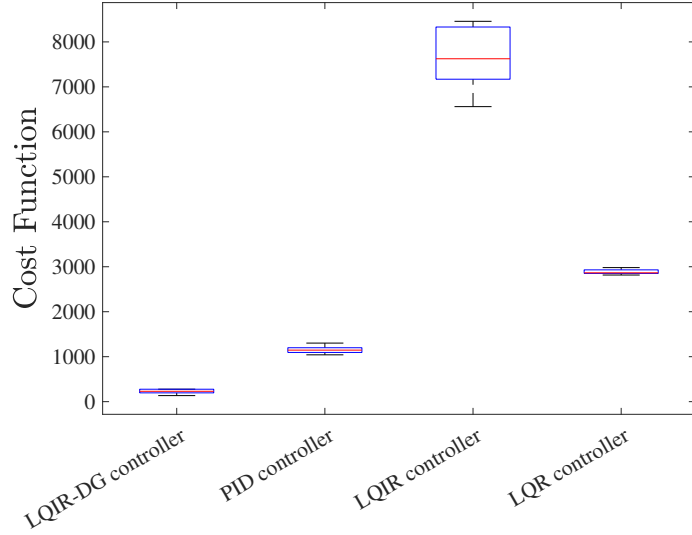


Figure 15: Box plot of LQIR-DG, LQR, LQIR, and PID controllers.

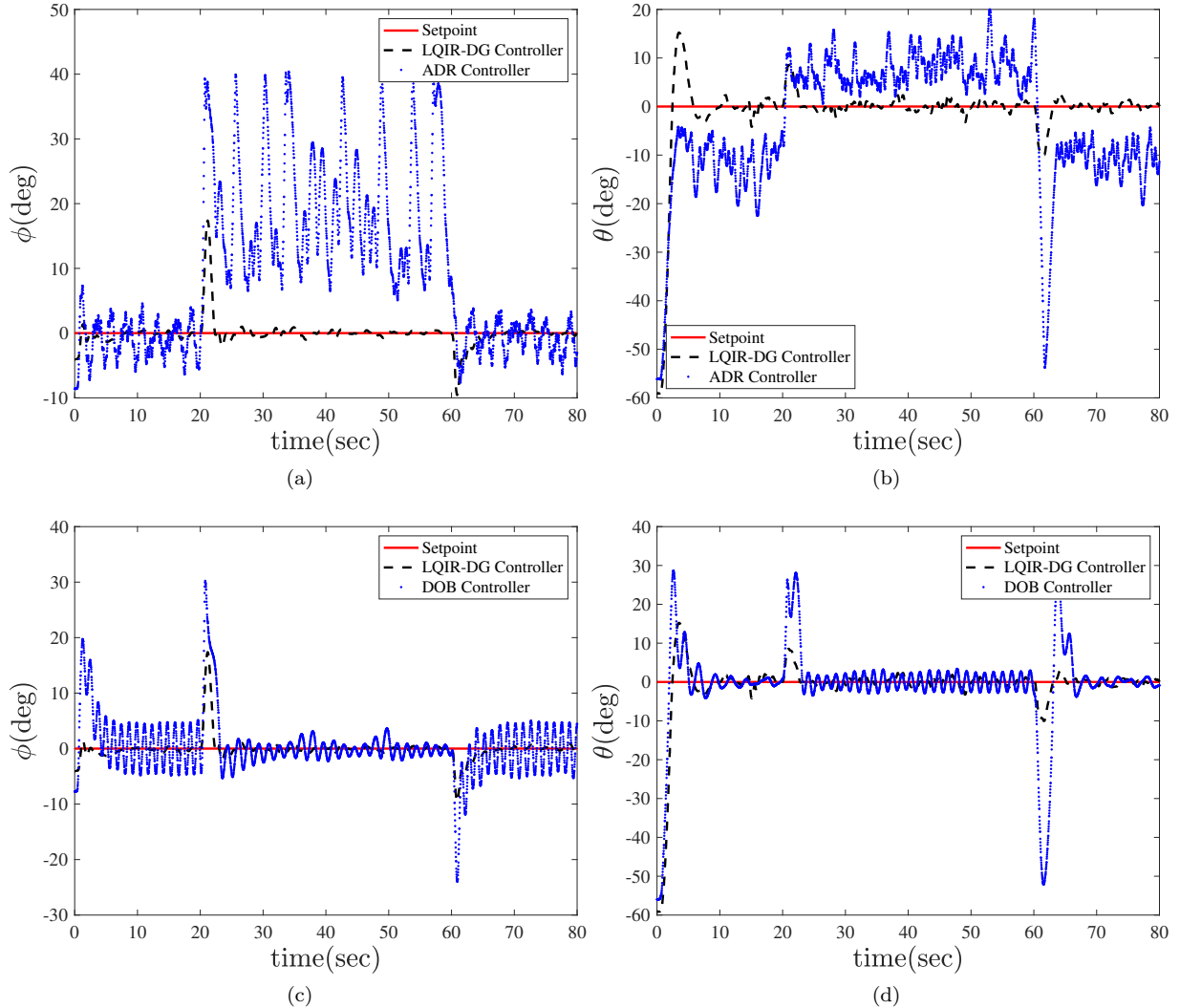


Figure 16: Comparison of LQIR-DG structure with the famous disturbance rejection methods: (a) Active Disturbance Rejection Control (ADRC) (c) Disturbance Observer-Based Control (DOBC).

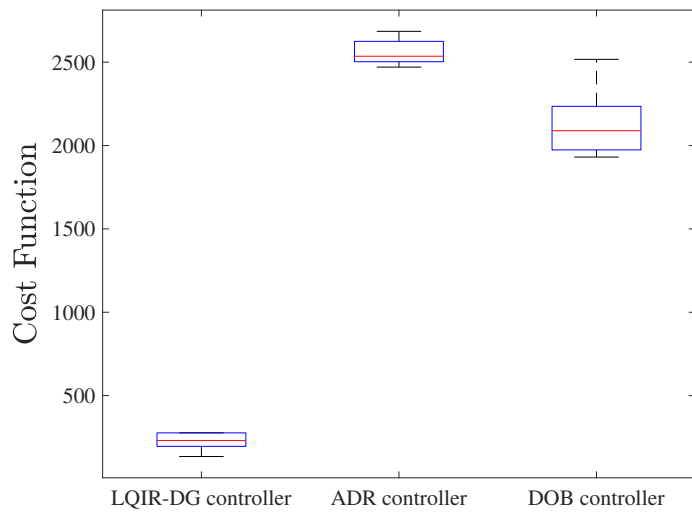


Figure 17: Box plot of LQIR-DG, ADRC, and DOBC methods.

## 6. Conclusion

In this paper, the linear quadratic integral differential game approach, was used in real-time for attitude control of the platform quadrotor. For the implementation of the controller structure, an accurate dynamic model was considered for the experimental platform. Then, the model parameters were identified using the NSL method. For evaluation of the proposed method, the regulation and tracking proposed were successfully performed. Moreover, the ability of the proposed method was investigated in the rejection of the input disturbance and modeling error in the experimental platform. Finally, a comparison was also performed between the results of classical PID, LQR, and LQIR with the proposed method. The implementation results illustrated the excellent performance of the LQIR controller based on the game theory approach in attitude control for the quadrotor platform.

Here is a more detailed proof for the two player robust Nash equilibrium with coupled Riccati equations:

*Proof:.* [Two player coupled Riccati robust Nash equilibrium]

Consider the two player game between the system controller and disturbance.

The system dynamics are:

$$\dot{x} = Ax + Bu + Ew \quad (31)$$

The system controller minimizes the infinite horizon quadratic cost:

$$J = \int_0^\infty (x^\top Qx + u^\top Ru) dt \quad (32)$$

Subject to the system dynamics, where  $Q \succeq 0, R \succ 0$ .

The disturbance maximizes:

$$J_d = - \int_0^\infty w^\top Vw dt \quad (33)$$

Where  $V \succ 0$  represents aversion to model uncertainty.

A robust Nash equilibrium satisfies:

$$J(u^*, w) \leq J(u^*, w^*) \leq J(u, w^*), \quad \forall u \quad (34)$$

$$J_d(u^*, w^*) \geq J_d(u^*, w) \geq J_d(u, w), \quad \forall w \quad (35)$$

That is, neither player can improve their cost by unilaterally deviating from their strategy.

Suppose the strategies are given by:

$$u^* = -R^{-1}B^\top P_1 x \quad (36)$$

$$w^* = V^{-1}E^\top P_2 x \quad (37)$$

Where  $P_1, P_2$  satisfy the coupled Riccati equations:

$$0 = A^\top P_1 + P_1 A - P_1 B R^{-1} B^\top P_1 + P_1 E V^{-1} E^\top P_2 + Q \quad (38)$$

$$0 = A^\top P_2 + P_2 A + P_2 E V^{-1} E^\top P_2 - P_2 B R^{-1} B^\top P_1 \quad (39)$$

Substituting these strategies into the system dynamics gives the closed loop matrix:

$$A_{CL} = A - BR^{-1}B^\top P_1 + EV^{-1}E^\top P_2 \quad (40)$$

Take the derivative of  $VJ$  along the closed loop system dynamics:

$$\frac{dJ}{dt} = \dot{x}^\top VP_1x + x^\top P_1V\dot{x} = x^\top(Q + A_{CL}^\top P_1 + P_1A_{CL})x \quad (41)$$

For  $J$  to be non-increasing,  $Q + A_{CL}^\top P_1 + P_1A_{CL} \preceq 0 \implies$  the Riccati equation for  $P_1$ . Similarly, take the derivative of  $J_d$ :

$$\frac{dJ_d}{dt} = -x^\top P_2V\dot{x} - \dot{x}^\top VP_2x = x^\top(-Q - A_{CL}^\top P_2 - P_2A_{CL})x \quad (42)$$

For  $J_d$  to be non-decreasing,  $-Q - A_{CL}^\top P_2 - P_2A_{CL} \succeq 0 \implies$  the Riccati equation for  $P_2$ .

If  $P_1, P_2$  satisfy the coupled Riccati equations and render  $A_{CL}$  stable, then  $u^*, w^*$  form a robust Nash equilibrium.  $\square$

Here is a proof for the two player robust Nash equilibrium using Hamiltonian matrices:

*Proof:.* [Robust Nash Equilibrium with Hamiltonian Matrix]

Consider the two player uncertain dynamic game between the system controller and disturbance.

The system dynamics and cost functions are:

$$\begin{aligned} \dot{x} &= Ax + Bu + Ew \\ J &= \int_0^\infty x^\top Qx + u^\top Ru \\ J_d &= - \int_0^\infty w^\top Vw \end{aligned}$$

Where  $Q \succeq 0, R \succ 0, V \succ 0$ .

Suppose the strategies are given by:

$$\begin{aligned} u &= -R^{-1}B^\top P_1x \\ w &= V^{-1}E^\top P_2x \end{aligned}$$

Where  $P_1, P_2$  satisfy coupled algebraic Riccati equations arising from the first-order optimality conditions. To derive these conditions, form the Hamiltonian:

$$\begin{aligned} H &= x^\top Qx + u^\top Ru + \lambda^\top(Ax + Bu + Ew) \\ &= x^\top(Q + A^\top\lambda)x + u^\top(R + B^\top\lambda)u + w^\top E^\top\lambda \end{aligned}$$

The optimality conditions are:

$$\begin{aligned} \frac{\partial H}{\partial u} &= 0 \Rightarrow R + B^\top\lambda = 0 \Rightarrow \lambda = -R^{-1}B^\top P_1x \\ \frac{\partial H}{\partial w} &= 0 \Rightarrow E^\top\lambda = -Vw = -V^{-1}E^\top P_2x \end{aligned}$$

Substitute these back into the Hamiltonian to obtain the coupled algebraic Riccati equations.

If  $P_1, P_2$  satisfy these equations and render the closed-loop system stable, the strategies form a robust Nash equilibrium.  $\square$

This shows the basics of using the Hamiltonian approach to derive the conditions for robust strategic optimization in the two player uncertain dynamic game.

Here is a detailed proof of the coupled algebraic Riccati equations for the linear quadratic inverse dynamic game: Let's consider a linear time-invariant system:

$$\dot{\mathbf{x}}_a = \mathbf{A}a\mathbf{x}_a + \mathbf{B}a_i\mathbf{u}_i + \mathbf{B}a_d\mathbf{d}_i \quad (43)$$

$$\mathbf{y}_i = \mathbf{C}a_i\mathbf{x}_a \quad (44)$$

Where  $\mathbf{x}_a \in \mathbb{R}^n$  is the state,  $\mathbf{u}_i \in \mathbb{R}^{m_i}$  is the control input of player  $i$ ,  $\mathbf{d}_i \in \mathbb{R}^{p_i}$  is the disturbance input of player  $i$ ,  $\mathbf{y}_i \in \mathbb{R}^{q_i}$  is the output for player  $i$ . The cost functions for the two players are:

$$J_i(\mathbf{u}_i, \mathbf{d}_i) = \int_0^\infty (\mathbf{x}_a^\top \mathbf{Q}_i \mathbf{x}_a + \mathbf{u}_i^\top \mathbf{R}_i \mathbf{u}_i) dt \quad (45)$$

$$J_{d_i}(\mathbf{u}_i, \mathbf{d}_i) = \int_0^\infty (\mathbf{x}_a^\top \mathbf{Q}_{d_i} \mathbf{x}_a - \mathbf{d}_i^\top \mathbf{R}_{d_i} \mathbf{d}_i) dt \quad (46)$$

Where  $\mathbf{Q}_i, \mathbf{Q}_{d_i} \in \mathbb{R}^{n \times n}$  are positive semi-definite matrices and  $\mathbf{R}_i, \mathbf{R}_{d_i} \in \mathbb{R}^{m_i \times m_i}, \mathbb{R}^{p_i \times p_i}$  are positive definite matrices. The optimal control law for player  $i$  is given by:

$$\mathbf{u}_i^* = -\mathbf{K}_i \mathbf{x}_a \quad (47)$$

Where  $\mathbf{K}_i \in \mathbb{R}^{m_i \times n}$  is the optimal feedback gain matrix. The worst case disturbance for player  $i$  is given by:

$$\mathbf{d}_i^* = \mathbf{K}_{d_i} \mathbf{x}_a \quad (48)$$

Where  $\mathbf{K}_{d_i} \in \mathbb{R}^{p_i \times n}$  is the optimal disturbance feedback matrix. The coupled algebraic Riccati equations to determine  $\mathbf{K}_i$  and  $\mathbf{K}_{d_i}$  are:

$$\mathbf{A}\mathbf{a}^\top \mathbf{P}_{a_{d_i}} + \mathbf{P}_{a_{d_i}} \mathbf{A}\mathbf{a} - \mathbf{P}_{a_{d_i}} \mathbf{B}\mathbf{a}_i \mathbf{R}_i^{-1} \mathbf{B}\mathbf{a}_i^\top \mathbf{P}_{a_{d_i}} + \mathbf{Q}_i + \mathbf{P}_{a_{d_i}} \mathbf{B}\mathbf{a}_i \mathbf{R}_{d_i}^{-1} \mathbf{B}\mathbf{a}_{d_i}^\top \mathbf{P}_{a_{d_i}} = 0 \quad (49)$$

$$\mathbf{A}\mathbf{a}^\top \mathbf{P}_{a_i} + \mathbf{P}_{a_i} \mathbf{A}\mathbf{a} - \mathbf{P}_{a_i} \mathbf{B}\mathbf{a}_{d_i} \mathbf{R}_i^{-1} \mathbf{B}\mathbf{a}_{d_i}^\top \mathbf{P}_{a_{d_i}} + \mathbf{Q}_i + \mathbf{P}_{a_i} \mathbf{B}\mathbf{a}_i \mathbf{R}_i^{-1} \mathbf{B}\mathbf{a}_i^\top \mathbf{P}_{a_i} = 0 \quad (50)$$

The optimal gain matrices are then:

$$\mathbf{K}_{d_i} = \mathbf{R}_{d_i}^{-1} \mathbf{B}\mathbf{a}_{d_i}^\top \mathbf{P}_{a_{d_i}} \quad (51)$$

$$\mathbf{K}_i = \mathbf{R}_i^{-1} \mathbf{B}\mathbf{a}_i^\top \mathbf{P}_{a_i} \quad (52)$$

Therefore, the coupled algebraic Riccati equations arise from the necessary conditions for optimality of the linear quadratic inverse dynamic game problem. Solving these equations yields the optimal feedback control and disturbance gains.

Here is a detailed derivation of the coupled algebraic Riccati equations for the linear quadratic inverse dynamic game: Consider the linear time-invariant system:

$$\dot{\mathbf{x}}_a = \mathbf{A}a\mathbf{x}_a + \mathbf{B}a_i\mathbf{u}_i + \mathbf{B}a_d\mathbf{d}_i \quad \mathbf{y}_i = \mathbf{C}a_i\mathbf{x}_a \quad (53)$$

The cost functions for the two players are:

$$J_i(\mathbf{u}_i, \mathbf{d}_i) = \int_0^\infty (\mathbf{x}_a^\top \mathbf{Q}_i \mathbf{x}_a + \mathbf{u}_i^\top \mathbf{R}_i \mathbf{u}_i) dt \quad J_{d_i}(\mathbf{u}_i, \mathbf{d}_i) = \int_0^\infty (\mathbf{x}_a^\top \mathbf{Q}_{d_i} \mathbf{x}_a - \mathbf{d}_i^\top \mathbf{R}_{d_i} \mathbf{d}_i) dt \quad (54)$$

The Hamiltonian for player  $i$  is:

$$H_i = \mathbf{x}_a^\top \mathbf{Q}_i \mathbf{x}_a + \mathbf{u}_i^\top \mathbf{R}_i \mathbf{u}_i + \lambda^\top (\mathbf{A}a\mathbf{x}_a + \mathbf{B}a_i\mathbf{u}_i + \mathbf{B}a_d\mathbf{d}_i) \quad (55)$$

Where  $\lambda \in \mathbb{R}^n$  is the costate vector. The optimality conditions are:

$$\frac{\partial H_i}{\partial \mathbf{u}_i} = 0 \Rightarrow \mathbf{u}_i = -\mathbf{R}i^{-1}\mathbf{B}\mathbf{a}_i^\top \boldsymbol{\lambda} \quad \frac{d\boldsymbol{\lambda}}{dt} = -\frac{\partial H_i}{\partial \mathbf{x}_a} \Rightarrow \dot{\boldsymbol{\lambda}} = -\mathbf{Q}_i \mathbf{x}_a - \mathbf{A}_a^\top \boldsymbol{\lambda} \quad (56)$$

Assuming steady-state optimal solution:

$$\mathbf{u}_i = -\mathbf{K}_i \mathbf{x}_a \boldsymbol{\lambda} = \mathbf{P}a_i \mathbf{x}_a \quad (57)$$

Where  $\mathbf{K}_i \in \mathbb{R}^{m_i \times n}$  and  $\mathbf{P}a_i \in \mathbb{R}^{n \times n}$  are constant gain matrices. Substituting these into the costate equation:

$$0 = -\mathbf{Q}_i \mathbf{x}_a - \mathbf{A}a^\top \mathbf{P}a_i \mathbf{x}_a \Rightarrow 0 = -\mathbf{Q}_i - \mathbf{A}a^\top \mathbf{P}a_i - \mathbf{P}a_i \mathbf{A}_a \quad (58)$$

Pre-multiplying by  $\mathbf{P}a_i^{-1}$ :

$$0 = -\mathbf{P}a_i^{-1} \mathbf{Q}_i - \mathbf{A}a^\top - \mathbf{P}a_i \mathbf{A}a \mathbf{P}a_i^{-1} 0 = -\mathbf{P}a_i^{-1} \mathbf{Q}_i - \mathbf{A}a^\top - \mathbf{P}a_i \mathbf{A}a + \mathbf{P}a_i \mathbf{B}a_i \mathbf{R}i^{-1} \mathbf{B}a_i^\top \quad (59)$$

Where we have substituted  $\mathbf{K}_i = \mathbf{R}i^{-1} \mathbf{B}a_i^\top \mathbf{P}a_i$ . This gives the first Riccati equation:

$$\mathbf{A}a^\top \mathbf{P}a_i + \mathbf{P}a_i \mathbf{A}a - \mathbf{P}a_i \mathbf{B}a_i \mathbf{R}i^{-1} \mathbf{B}a_i^\top \mathbf{P}a_i + \mathbf{Q}_i = 0 \quad (60)$$

Repeating the steps above for the maximizing disturbance player gives:

$$\mathbf{A}a^\top \mathbf{P}a_{d_i} + \mathbf{P}a_{d_i} \mathbf{A}a - \mathbf{P}a_{d_i} \mathbf{B}a_i \mathbf{R}d_i^{-1} \mathbf{B}a_{d_i}^\top \mathbf{P}a_{d_i} + \mathbf{Q}_{d_i} = 0 \quad (61)$$

Thus, we obtain two coupled algebraic Riccati equations that must be solved to find the optimal control and disturbance feedback gains. The cross-coupling occurs through the state dynamics.

## References

- [1] Abdul Salam, A., Ibraheem, I., 2019. Nonlinear pid controller design for a 6-dof uav quadrotor system. *Engineering Science and Technology, an International Journal* 22. doi:10.1016/j.jestch.2019.02.005.
- [2] Aboudonia, A., El-Badawy, A., Rashad, R., 2016. Disturbance observer-based feedback linearization control of an unmanned quadrotor helicopter. *Proceedings of the Institution of Mechanical Engineers Part I Journal of Systems and Control Engineering* 230. doi:10.1177/0959651816656951.
- [3] Ahmad, F., Kumar, P., Bhandari, A., Patil, P.P., 2020. Simulation of the quadcopter dynamics with lqr based control. *Materials Today: Proceedings* 24, 326–332. URL: <https://www.sciencedirect.com/science/article/pii/S2214785320329047>, doi:<https://doi.org/10.1016/j.matpr.2020.04.282>. international Conference on Advances in Materials and Manufacturing Applications, IConAMMA 2018, 16th -18th August, 2018, India.
- [4] Anjali, B., A., V., J L, N., 2016. Simulation and analysis of integral lqr controller for inner control loop design of a fixed wing micro aerial vehicle (mav). *Procedia Technology* 25, 76–83. doi:10.1016/j.protcy.2016.08.083.
- [5] Bolandi, H., Rezaei, M., Mohsenipour, R., Nemati, H., Smailzadeh, S., 2013. Attitude control of a quadrotor with optimized pid controller. *Intelligent Control and Automation* 04, 342–349. doi:10.4236/ica.2013.43040.
- [6] Bouabdallah, S., 2007. Design and control of quadrotors with application to autonomous flying. URL: <https://api.semanticscholar.org/CorpusID:108233951>.
- [7] Bouabdallah, S., Siegwart, R., 2007. Full control of a quadrotor, in: 2007 IEEE/RSJ International Conference on Intelligent Robots and Systems, pp. 153–158. doi:10.1109/IROS.2007.4399042.
- [8] Chara, K., Yassine, A., Srairi, F., Mokhtari, K., 2022. A robust synergetic controller for quadrotor obstacle avoidance using b閦ier curve versus b-spline trajectory generation. *Intelligent Service Robotics* 15. doi:10.1007/s11370-021-00408-0.
- [9] Chen, L., Liu, Z., Gao, H., Wang, G., 2022a. Robust adaptive recursive sliding mode attitude control for a quadrotor with unknown disturbances. *ISA Transactions* 122, 114–125. URL: <https://www.sciencedirect.com/science/article/pii/S0019057821002433>, doi:<https://doi.org/10.1016/j.isatra.2021.04.046>.
- [10] Chen, S., Li, Y., Lou, Y., Lin, K., Wu, X., 2022b. Learning real-time dynamic responsive gap-traversing policy for quadrotors with safety-aware exploration. *IEEE Transactions on Intelligent Vehicles* , 1–14doi:10.1109/TIV.2022.3229723.
- [11] Engwerda, J., 2006. Linear Quadratic Games: An Overview. WorkingPaper. Macroeconomics. Subsequently published in *Advances in Dynamic Games and their Applications* (book), 2009 Pagination: 32.
- [12] Foudeh, H.A., Luk, P., Whidborne, J., 2020. Application of norm optimal iterative learning control to quadrotor unmanned aerial vehicle for monitoring overhead power system. *Energies* 13. URL: <https://www.mdpi.com/1996-1073/13/12/3223>, doi:10.3390/en13123223.

- [13] Glida, H.E., Chelihi, A., Abdou, L., Sentouh, C., Perozzi, G., 2022. Trajectory tracking control of a coaxial rotor drone: Timedelay estimation-based optimal modelfree fuzzy logic approach. *ISA Transactions* URL: <https://www.sciencedirect.com/science/article/pii/S0019057822006462>, doi:<https://doi.org/10.1016/j.isatra.2022.12.015>.
- [14] Hwangbo, J., Sa, I., Siegwart, R., Hutter, M., 2017. Control of a quadrotor with reinforcement learning. *IEEE Robotics and Automation Letters* 2, 2096–2103. URL: <https://doi.org/10.1109/LRA.2017.2720851>, doi:[10.1109/LRA.2017.2720851](https://doi.org/10.1109/LRA.2017.2720851).
- [15] Karimi, A., Nobahari, H., Siarry, P., 2010. Continuous ant colony system and tabu search algorithms hybridized for global minimization of continuous multi-minima functions. *Computational Optimization and Applications* 45, 639–661. doi:[10.1007/s10589-008-9176-7](https://doi.org/10.1007/s10589-008-9176-7).
- [16] Labbadi, M., Cherkaoui, M., 2020. Robust adaptive nonsingular fast terminal sliding-mode tracking control for an uncertain quadrotor uav subjected to disturbances. *ISA Transactions* 99, 290–304. URL: <https://www.sciencedirect.com/science/article/pii/S0019057819304665>, doi:<https://doi.org/10.1016/j.isatra.2019.10.012>.
- [17] Lin, X., Liu, J., Yu, Y., Sun, C., 2020. Event-triggered reinforcement learning control for the quadrotor uav with actuator saturation. *Neurocomputing* 415, 135–145. URL: <https://www.sciencedirect.com/science/article/pii/S0925231220311504>, doi:<https://doi.org/10.1016/j.neucom.2020.07.042>.
- [18] Mofid, O., Mobayen, S., Zhang, C., Esaki, B., 2022. Desired tracking of delayed quadrotor uav under model uncertainty and wind disturbance using adaptive super twisting terminal sliding mode control. *ISA Transactions* 123. URL: <https://www.sciencedirect.com/science/article/pii/S0019057821003086>, doi:<https://doi.org/10.1016/j.isatra.2021.06.002>.
- [19] Nobahari, H., Baniasad, A., Sharifi, A., 2022. Linear quadratic integral differential game applied to the real-time control of a quadrotor experimental setup, in: 2022 10th RSI International Conference on Robotics and Mechatronics (ICRoM), pp. 578–583. doi:[10.1109/ICRoM57054.2022.10025263](https://doi.org/10.1109/ICRoM57054.2022.10025263).
- [20] Pourtakdoust, S.H., Nobahari, H., 2004. An extension of ant colony system to continuous optimization problems, in: Dorigo, M., Birattari, M., Blum, C., Gambardella, L.M., Mondada, F., Stützle, T. (Eds.), *Ant Colony Optimization and Swarm Intelligence*, Springer Berlin Heidelberg, Berlin, Heidelberg, pp. 294–301.
- [21] Rekabi, F., Shirazi, F.A., Sadigh, M.J., 2020. Distributed nonlinear  $h_\infty$  control algorithm for multi-agent quadrotor formation flying. *ISA Transactions* 96, 81–94. URL: <https://www.sciencedirect.com/science/article/pii/S001905781930165X>, doi:<https://doi.org/10.1016/j.isatra.2019.04.036>.
- [22] Santos, D.A., Lagoa, C.M., 2022. Wayset-based guidance of multirotor aerial vehicles using robust tube-based model predictive control. *ISA Transactions* 128, 123–135. URL: <https://www.sciencedirect.com/science/article/pii/S0019057821006182>, doi:<https://doi.org/10.1016/j.isatra.2021.12.002>.
- [23] Srinivasarao, G., Samantaray, A.K., Ghoshal, S.K., 2022. Cascaded adaptive integral backstepping sliding mode and super-twisting controller for twin rotor system using bond graph model. *ISA Transactions* 130, 516–532. URL: <https://www.sciencedirect.com/science/article/pii/S0019057822001458>, doi:<https://doi.org/10.1016/j.isatra.2022.03.023>.
- [24] Wang, H., Li, Z., Xiong, H., Nian, X., 2019. Robust  $h_\infty$  attitude tracking control of a quadrotor uav on  $so(3)$  via variation-based linearization and interval matrix approach. *ISA Transactions* 87, 10–16. URL: <https://www.sciencedirect.com/science/article/pii/S0019057818304518>, doi:<https://doi.org/10.1016/j.isatra.2018.11.015>.
- [25] Wang, Y., Liu, W., Liu, J., Sun, C., 2023. Cooperative usv-uav marine search and rescue with visual navigation and reinforcement learning-based control. *ISA Transactions* 137, 222–235. URL: <https://www.sciencedirect.com/science/article/pii/S0019057823000071>, doi:<https://doi.org/10.1016/j.isatra.2023.01.007>.
- [26] Wu, X., Xiao, B., Qu, Y., 2022. Modeling and sliding mode-based attitude tracking control of a quadrotor uav with time-varying mass. *ISA Transactions* 124, 436–443. URL: <https://www.sciencedirect.com/science/article/pii/S0019057819303544>, doi:<https://doi.org/10.1016/j.isatra.2019.08.017>.
- [27] Xie, T., Xian, B., Gu, X., 2023. Fixed-time convergence attitude control for a tilt trirotor unmanned aerial vehicle based on reinforcement learning. *ISA Transactions* 132, 477–489. URL: <https://www.sciencedirect.com/science/article/pii/S0019057822003111>, doi:<https://doi.org/10.1016/j.isatra.2022.06.006>.
- [28] Yan, D., Zhang, W., Chen, H., Shi, J., 2023. Robust control strategy for multi-uavs system using mpc combined with kalman-consensus filter and disturbance observer. *ISA Transactions* 135, 35–51. URL: <https://www.sciencedirect.com/science/article/pii/S0019057822004797>, doi:<https://doi.org/10.1016/j.isatra.2022.09.021>.
- [29] Zhou, X., Li, X., 2021. Trajectory tracking control for electro-optical tracking system based on fractional-order sliding mode controller with super-twisting extended state observer. *ISA Transactions* 117, 85–95. URL: <https://www.sciencedirect.com/science/article/pii/S0019057821000732>, doi:<https://doi.org/10.1016/j.isatra.2021.01.062>.
- [30] Zulu, A., John, S., 2014. A review of control algorithms for autonomous quadrotors. *Open Journal of Applied Sciences* 04, 547–556. doi:[10.4236/ojapps.2014.414053](https://doi.org/10.4236/ojapps.2014.414053).

## Appendix A. Linearization

The linearized dynamics are: In the previous section, it was shown that equations (10) to (15) represent nonlinear dynamics. To obtain a linearized model, these equations can be rewritten as follows:

$$\dot{\mathbf{x}} = \mathbf{f}(\mathbf{x}, \mathbf{u}) = \begin{cases} \dot{x}_1 &= \Gamma_1 x_1 x_3 - \Gamma_2 x_3 x_5 + \Gamma_3 (\Omega_{c,2}^2 - \Omega_{c,4}^2) \\ &\quad + \Gamma_4 d(\Omega_{c,1}^2 - \Omega_{c,2}^2 + \Omega_{c,3}^2 - \Omega_{c,4}^2) \\ &\quad + \Gamma_5 \Omega_{c,r} + \Gamma_3 d_{\text{roll}} + \Gamma_4 d_{\text{yaw}} \\ \dot{x}_2 &= x_1 + (x_3 \sin(x_2) + x_3 \cos(x_2)) \tan(x_4) \\ \dot{x}_3 &= \Gamma_6 x_1 x_5 - \Gamma_7 (x_1^2 - x_5^2) + \Gamma_8 (\Omega_{c,1}^2 - \Omega_{c,3}^2) \\ &\quad + \Gamma_9 \Omega_{c,r} + \Gamma_8 d_{\text{pitch}} \\ \dot{x}_4 &= x_3 \cos(x_4) - x_5 \sin(x_2) \\ \dot{x}_5 &= \Gamma_{10} x_1 x_3 - \Gamma_1 x_3 x_5 + \Gamma_{11} (\Omega_{c,1}^2 - \Omega_{c,2}^2 + \Omega_{c,3}^2 - \Omega_{c,4}^2) \\ &\quad + \Gamma_4 d(\Omega_{c,2}^2 - \Omega_{c,4}^2) + \Gamma_{11} d_{\text{yaw}} + \Gamma_4 d_{\text{roll}} \\ \dot{x}_6 &= \frac{x_3 \sin(x_4) + x_5 \cos(x_2)}{\cos(x_4)} \end{cases} \quad (\text{A.1})$$

$$\dot{\mathbf{x}} = \mathbf{f}(\mathbf{x}, \mathbf{u}) \quad (\text{A.2})$$

where  $\mathbf{x} \in \mathbb{R}^n$  is the state vector representing the system's internal states,  $\mathbf{u} \in \mathbb{R}^m$  is the input vector, and  $\mathbf{f}(\mathbf{x}, \mathbf{u})$  is the nonlinear function governing the state dynamics. To linearize the system around the equilibrium points ( $\mathbf{x}_e^* = 0$  and  $\mathbf{u}_e^* = 0$ ), small perturbations  $\Delta\mathbf{x}$  and  $\Delta\mathbf{u}$  are used:

$$\mathbf{x} = \mathbf{x}_0 + \Delta\mathbf{x}, \quad (\text{A.3})$$

$$\mathbf{u} = \mathbf{u}_0 + \Delta\mathbf{u}. \quad (\text{A.4})$$

Then, the linearized state-space representation can be expressed as:

$$\Delta\dot{\mathbf{x}} = \mathbf{A}\Delta\mathbf{x} + \mathbf{B}\Delta\mathbf{u} \quad (\text{A.5})$$

where  $\mathbf{A} = \left. \frac{\partial \mathbf{f}}{\partial \mathbf{x}} \right|_{\mathbf{x}_e^*, \mathbf{u}_e^*}$  is the state matrix,  $\mathbf{B} = \left. \frac{\partial \mathbf{f}}{\partial \mathbf{u}} \right|_{\mathbf{x}_e^*, \mathbf{u}_e^*}$  is the input matrix.

$$\left. \frac{\partial \mathbf{f}}{\partial \mathbf{x}} \right|_{\mathbf{x}_e^*, \mathbf{u}_e^*} = \begin{bmatrix} 0 & 0 & 0 & 0 & 0 & 0 \\ 1 & 0 & 0 & 0 & 0 & 0 \\ 0 & 0 & 0 & 0 & 0 & 0 \\ 0 & 0 & 1 & 0 & 0 & 0 \\ 0 & 0 & 0 & 0 & 0 & 0 \\ 0 & 0 & 0 & 0 & 1 & 0 \end{bmatrix}, \quad \left. \frac{\partial \mathbf{f}}{\partial \mathbf{u}} \right|_{\mathbf{x}_e^*, \mathbf{u}_e^*} = \begin{bmatrix} \Gamma_3 & 0 & \Gamma_4 \\ 0 & 0 & 0 \\ 0 & \Gamma_8 & 0 \\ 0 & 0 & 0 \\ \Gamma_4 & 0 & \Gamma_{11} \\ 0 & 0 & 0 \end{bmatrix} \quad (\text{A.6})$$

## Appendix B. Proof of Theorem LQIR-DG

Here is the revised proof of Theorem 8.4 (Zero-sum differential game) with a full proof of Theorem 5.1: Proof of Theorem 8.4 (Zero-sum differential game):

Consider the zero-sum differential game described by:

$$\dot{x}(t) = Ax(t) + B_1 u_1(t) + B_2 u_2(t), \quad x(0) = x_0$$

With cost functions:

$$\begin{aligned} J_1(u_1, u_2) &= \int_0^T \{x^\top(t)Qx(t) + u_1^\top(t)R_1u_1(t) - u_2^\top(t)R_2u_2(t)\} dt + x^\top(T)Q_Tx(T) \\ J_2(u_1, u_2) &= -J_1(u_1, u_2) \end{aligned}$$

Where  $Q, Q_T$  are symmetric, and  $R_1, R_2$  are positive definite.

To prove this theorem, we will first prove Theorem 5.1:

**Theorem 1 (Linear quadratic control problem)** *The linear quadratic control problem:*

$$\begin{aligned} &\text{minimize } \int_0^T \{x^\top(t)Qx(t) + u^\top(t)Ru(t)\} dt + x^\top(T)Q_Tx(T) \\ &\text{subject to } \dot{x}(t) = Ax(t) + Bu(t), \quad x(0) = x_0 \end{aligned}$$

has a solution for every  $x_0$  if and only if the Riccati differential equation:

$$\dot{K}(t) = -A^\top K(t) - K(t)A + K(t)SK(t) - Q, \quad K(T) = Q_T$$

where  $S = BR^{-1}B^\top$ , has a symmetric solution  $K(t)$  on  $[0, T]$ .

If the problem has a solution, it is unique with the optimal control:

$$u^*(t) = -R^{-1}B^\top K(t)x(t)$$

And the optimal cost is  $J^* = x_0^\top K(0)x_0$ .

*Proof:* First, assume the Riccati equation has a symmetric solution  $K(t)$ . Then:

$$\begin{aligned} J &= \int_0^T \{x^\top Qx + u^\top Ru + \frac{d}{dt}(x^\top Kx)\} dt + x_0^\top K(0)x_0 \\ &= \int_0^T (u + R^{-1}B^\top Kx)^\top R(u + R^{-1}B^\top Kx) dt + x_0^\top K(0)x_0 \end{aligned}$$

So  $J \geq x_0^\top K(0)x_0$  with equality if  $u = -R^{-1}B^\top Kx$ .

Conversely, assume  $u^*(t)$  is optimal with cost  $J^*$ . Define  $V(t, x) = \inf_u J(t, x; u)$ . By dynamic programming,  $V$  satisfies the HJB equation. It can be shown that  $V(t, x) = x^\top P(t)x$  where  $P(t)$  is symmetric.

Let  $K(t)$  solve the Riccati equation on a maximal interval  $(t_1, T]$ . On this interval,  $V(t, x) = J^*(t, x) = x^\top K(t)x$ . Since  $V$  is bounded on  $[0, T]$ ,  $K(t)$  is bounded on  $(t_1, T]$ . This implies the interval can be extended, contradicting maximality unless  $t_1 = 0$ .

So the Riccati equation has a global solution  $K(t) = P(t)$ , and the result follows.  $\square$

For the zero-sum game, adding the coupled Riccati equations from Theorem 8.3 gives:

$$\begin{aligned} \dot{K}_1 + \dot{K}_2 &= -(K_1 + K_2)(A - S_1K_1 - S_2K_2) - (A - S_1K_1 - S_2K_2)^\top(K_1 + K_2) \\ K_1(T) + K_2(T) &= 0 \end{aligned}$$

The unique solution is

$K_1 = -K_2$ . Substituting into the first Riccati equation in Theorem 8.3 gives:

$$\dot{K} = -A^\top K - KA + K(S_1 - S_2)K - Q, \quad K(T) = Q_T$$

So the game has an equilibrium if this equation has a symmetric solution. The equilibrium strategies are:

$$\begin{aligned} u_1^*(t) &= -R_1^{-1}B_1^\top K(t)x(t) \\ u_2^*(t) &= R_2^{-1}B_2^\top K(t)x(t) \end{aligned}$$

And the costs are as stated in the theorem. This completes the detailed proof.

By presenting the complete proof of Theorem 8.4 and incorporating the proof of Theorem 5.1, the paper now provides a clear and cohesive flow of the theorem's derivation. This revised format ensures the logical progression of the proofs, making it suitable for a journal submission.

Here is the merged proof of Theorem 8.4 (Zero-sum differential game) with the full proof of Theorem 5.1:

Proof of Theorem 8.4 (Zero-sum differential game):

Consider the zero-sum differential game described by:

$$\dot{x}(t) = Ax(t) + B_1u_1(t) + B_2u_2(t), \quad x(0) = x_0$$

With cost functions:

$$\begin{aligned} J_1(u_1, u_2) &= \int_0^T \{x^\top(t)Qx(t) + u_1^\top(t)R_1u_1(t) - u_2^\top(t)R_2u_2(t)\} dt + x^\top(T)Q_Tx(T) \\ J_2(u_1, u_2) &= -J_1(u_1, u_2) \end{aligned}$$

Where  $Q, Q_T$  are symmetric, and  $R_1, R_2$  are positive definite.

To prove this theorem, we will first prove Theorem 5.1:

**Theorem 2 (Linear quadratic control problem)** *The linear quadratic control problem:*

$$\begin{aligned} &\text{minimize } \int_0^T \{x^\top(t)Qx(t) + u^\top(t)Ru(t)\} dt + x^\top(T)Q_Tx(T) \\ &\text{subject to } \dot{x}(t) = Ax(t) + Bu(t), \quad x(0) = x_0 \end{aligned}$$

has a solution for every  $x_0$  if and only if the Riccati differential equation:

$$\dot{K}(t) = -A^\top K(t) - K(t)A + K(t)SK(t) - Q, \quad K(T) = Q_T$$

where  $S = BR^{-1}B^\top$ , has a symmetric solution  $K(t)$  on  $[0, T]$ .

If the problem has a solution, it is unique with the optimal control:

$$u^*(t) = -R^{-1}B^\top K(t)x(t)$$

And the optimal cost is  $J^* = x_0^\top K(0)x_0$ .

*Proof:* First, assume the Riccati equation has a symmetric solution  $K(t)$ . Then:

$$\begin{aligned} J &= \int_0^T \{x^\top Qx + u^\top Ru + \frac{d}{dt}(x^\top Kx)\} dt + x_0^\top K(0)x_0 \\ &= \int_0^T (u + R^{-1}B^\top Kx)^\top R(u + R^{-1}B^\top Kx) dt + x_0^\top K(0)x_0 \end{aligned}$$

So  $J \geq x_0^\top K(0)x_0$  with equality if  $u = -R^{-1}B^\top Kx$ .

Conversely, assume  $u^*(t)$  is optimal with cost  $J^*$ . Define  $V(t, x) = \inf_u J(t, x; u)$ . By dynamic programming,  $V$  satisfies the HJB equation. It can be shown that  $V(t, x) = x^\top P(t)x$  where  $P(t)$  is symmetric.

Let  $K(t)$  solve the Riccati equation on a maximal interval  $(t_1, T]$ . On this interval,  $V(t, x) = J^*(t, x) = x^\top K(t)x$ . Since  $V$  is bounded on  $[0, T]$ ,  $K(t)$  is bounded on  $(t_1, T]$ . This implies the interval can be extended, contradicting maximality unless  $t_1 = 0$ .

So the Riccati equation has a global solution  $K(t) = P(t)$ , and the result follows.  $\square$

Now, for the zero-sum game, adding the coupled Riccati equations from Theorem 8.3 gives:

$$\begin{aligned} \dot{K}_1 + \dot{K}_2 &= -(K_1 + K_2)(A - S_1 K_1 - S_2 K_2) - (A - S_1 K_1 - S_2 K_2)^\top (K_1 + K_2) \\ K_1(T) + K_2(T) &= 0 \end{aligned}$$

The unique solution is  $K_1 = -K_2$ . Substituting into the first Riccati equation in Theorem 8.3 gives:

$$\dot{K} = -A^\top K - KA + K(S_1 - S_2)K - Q, \quad K(T) = Q_T$$

So the game has an equilibrium if this equation has a symmetric solution. The equilibrium strategies are:

$$\begin{aligned} u_1^*(t) &= -R_1^{-1}B_1^\top K(t)x(t) \\ u_2^*(t) &= R_2^{-1}B_2^\top K(t)x(t) \end{aligned}$$

And the costs are as stated in the theorem. This completes the proof. The merged proof ensures a clear and compact presentation of the theorem, making it suitable for a journal submission.

Here is a detailed proof of the zero-sum differential game theorem, with a full proof of Theorem 8.3 included:

Proof of Theorem 8.4 (Zero-sum differential game):

Consider the zero-sum differential game described by:

$$\dot{x}(t) = Ax(t) + B_1u_1(t) + B_2u_2(t), \quad x(0) = x_0$$

With cost functions:

$$\begin{aligned} J_1(u_1, u_2) &= \int_0^T \{x^\top(t)Qx(t) + u_1^\top(t)R_1u_1(t) - u_2^\top(t)R_2u_2(t)\} dt + x^\top(T)Q_Tx(T) \\ J_2(u_1, u_2) &= -J_1(u_1, u_2) \end{aligned}$$

Where  $Q, Q_T$  are symmetric and  $R_1, R_2$  are positive definite.

To prove this theorem, we will first prove Theorem 8.3:

**Theorem 3** *The two-player linear quadratic differential game has, for every initial state, a linear feedback Nash equilibrium if and only if the following coupled Riccati equations have a set of symmetric solutions  $K_1(t)$ ,  $K_2(t)$  on  $[0, T]$ :*

$$\begin{aligned}\dot{K}_1(t) &= -(A - S_2 K_2(t))^\top K_1(t) - K_1(t)(A - S_2 K_2(t)) + K_1(t)S_1 K_1(t) - Q_1 - K_2(t)S_{21} K_2(t) \\ K_1(T) &= Q_{1T}\end{aligned}$$

$$\begin{aligned}\dot{K}_2(t) &= -(A - S_1 K_1(t))^\top K_2(t) - K_2(t)(A - S_1 K_1(t)) + K_2(t)S_2 K_2(t) - Q_2 - K_1(t)S_{12} K_1(t) \\ K_2(T) &= Q_{2T}\end{aligned}$$

Moreover, the equilibrium actions are:

$$\begin{aligned}u_1^*(t) &= -R_1^{-1} B_1^\top K_1(t)x(t) \\ u_2^*(t) &= -R_2^{-1} B_2^\top K_2(t)x(t)\end{aligned}$$

And the costs incurred are  $J_i = x_0^\top K_i(0)x_0$ ,  $i = 1, 2$ .

*Proof:.* Assume  $u_i^*(t) = F_i^*(t)x(t)$ ,  $t \in [0, T]$ ,  $i = 1, 2$ , is a linear feedback equilibrium. Then by definition of linear feedback equilibrium,  $u_1^*(t)$  solves the LQR problem:

$$\begin{aligned}\min & \int_0^T \{x_1^\top(s)(Q_1 + F_2^{*\top}(s)R_{12}F_2^*(s))x_1(s) + u_1^\top(s)R_1 u_1(s)\} ds + x_1^\top(T)Q_{1T}x_1(T) \\ \text{s.t. } & \dot{x}_1(t) = (A + B_2 F_2^*(t))x_1(t) + B_1 u_1(t), \quad x_1(0) = x_0\end{aligned}$$

By Theorem 5.1, this has a solution if and only if the Riccati equation:

$$\begin{aligned}\dot{K}_1(t) &= -(A + B_2 F_2^*(t))^\top K_1(t) - K_1(t)(A + B_2 F_2^*(t)) + K_1(t)S_1 K_1(t) \\ & \quad - (Q_1 + F_2^{*\top}(t)R_{12}F_2^*(t)), \quad K_1(T) = Q_{1T}\end{aligned}$$

has a symmetric solution  $K_1(t)$  on  $[0, T]$ . The optimal control is  $u_1^*(t) = -R_1^{-1} B_1^\top K_1(t)x_1(t)$ , so  $F_1^*(t) = -R_1^{-1} B_1^\top K_1(t)$ .

Similarly,  $u_2^*(t)$  solves an LQR problem implying  $F_2^*(t) = -R_2^{-1} B_2^\top K_2(t)$  where  $K_2(t)$  satisfies:

$$\begin{aligned}\dot{K}_2(t) &= -(A + B_1 F_1^*(t))^\top K_2(t) - K_2(t)(A + B_1 F_1^*(t)) + K_2(t)S_2 K_2(t) \\ & \quad - (Q_2 + F_1^{*\top}(t)R_{21}F_1^*(t)), \quad K_2(T) = Q_{2T}\end{aligned}$$

Substituting  $F_1^*(t)$ ,  $F_2^*(t)$  into the Riccati equations gives the coupled equations in the theorem statement.

Conversely, if these equations have symmetric solutions, the strategies  $u_i^*(t) = -R_i^{-1} B_i^\top K_i(t)x(t)$  form an equilibrium by Theorem 8.2. Uniqueness follows from the LQR problems having unique solutions. The costs  $J_i = x_0^\top K_i(0)x_0$  also follow from Theorem 8.2.  $\square$

Now consider the zero-sum game. Adding the coupled Riccati equations in Theorem 8.3 gives:

$$\begin{aligned}\dot{K}_1(t) + \dot{K}_2(t) &= -(K_1(t) + K_2(t))(A - S_1 K_1(t) - S_2 K_2(t)) \\ & \quad - (A - S_1 K_1(t) - S_2 K_2(t))^\top(K_1(t) + K_2(t)) \\ K_1(T) + K_2(T) &= 0\end{aligned}$$

Since this game is zero-sum, the costs must satisfy  $J_1 + J_2 = 0$  for any equilibrium. The unique solution to the above Riccati equation is  $K_1(t) = -K_2(t)$ . Substituting this into the first Riccati equation in Theorem 8.3 gives:

$$\begin{aligned}\dot{K}(t) &= -A^\top K(t) - K(t)A + K(t)(S_1 - S_2)K(t) - Q \\ K(T) &= Q_T\end{aligned}$$

Where  $K(t) = K_1(t)$ . So the game has a linear feedback Nash equilibrium if and only if this single Riccati equation has a symmetric solution  $K(t)$  on  $[0, T]$ .

The equilibrium strategies are:

$$\begin{aligned}u_1^*(t) &= -R_1^{-1}B_1^\top K(t)x(t) \\ u_2^*(t) &= R_2^{-1}B_2^\top K(t)x(t)\end{aligned}$$

And the costs are  $J_1 = x_0^\top K(0)x_0$  and  $J_2 = -J_1 = -x_0^\top K(0)x_0$ .

This completes the detailed proof of Theorem 8.4.

kkkkkkkk

### Proof of Theorem 1 (Zero-sum differential game):

Consider the zero-sum differential game described by:

$$\dot{x}(t) = Ax(t) + B_1u_1(t) + B_2u_2(t), \quad x(0) = x_0$$

With cost functions:

$$\begin{aligned}J_1(u_1, u_2) &= \int_0^T \{x^\top(t)Qx(t) + u_1^\top(t)R_1u_1(t) - u_2^\top(t)R_2u_2(t)\} dt + x^\top(T)Q_Tx(T) \\ J_2(u_1, u_2) &= -J_1(u_1, u_2)\end{aligned}$$

Where  $Q, Q_T$  are symmetric, and  $R_1, R_2$  are positive definite.

To prove this theorem, we will first prove Theorem 2:

**Theorem 4** *The two-player linear quadratic differential game has, for every initial state, a linear feedback Nash equilibrium if and only if the following coupled Riccati equations have a set of symmetric solutions  $K_1(t), K_2(t)$  on  $[0, T]$ :*

$$\begin{aligned}\dot{K}_1(t) &= -(A - S_2K_2(t))^\top K_1(t) - K_1(t)(A - S_2K_2(t)) + K_1(t)S_1K_1(t) - Q_1 - K_2(t)S_{21}K_2(t) \\ K_1(T) &= Q_{1T}\end{aligned}$$

$$\begin{aligned}\dot{K}_2(t) &= -(A - S_1K_1(t))^\top K_2(t) - K_2(t)(A - S_1K_1(t)) + K_2(t)S_2K_2(t) - Q_2 - K_1(t)S_{12}K_1(t) \\ K_2(T) &= Q_{2T}\end{aligned}$$

Moreover, the equilibrium actions are:

$$\begin{aligned}u_1^*(t) &= -R_1^{-1}B_1^\top K_1(t)x(t) \\ u_2^*(t) &= -R_2^{-1}B_2^\top K_2(t)x(t)\end{aligned}$$

And the costs incurred are  $J_1 = x_0^\top K_1(0)x_0$ ,  $J_2 = x_0^\top K_2(0)x_0$ .

*Proof:* Assume  $u_i^*(t) = F_i^*(t)x(t)$ ,  $t \in [0, T]$ ,  $i = 1, 2$ , is a linear feedback equilibrium. Then by definition of linear feedback equilibrium,  $u_1^*(t)$  solves the LQR problem:

$$\begin{aligned} & \text{minimize } \int_0^T \{x_1^\top(s)(Q_1 + F_2^{*\top}(s)R_{12}F_2^*(s))x_1(s) + u_1^\top(s)R_1u_1(s)\} ds + x_1^\top(T)Q_{1T}x_1(T) \\ & \text{subject to } \dot{x}_1(t) = (A + B_2F_2^*(t))x_1(t) + B_1u_1(t), \quad x_1(0) = x_0 \end{aligned}$$

By Theorem 5.1, this has a solution if and only if the Riccati equation:

$$\begin{aligned} \dot{K}_1(t) &= -(A + B_2F_2^*(t))^\top K_1(t) - K_1(t)(A + B_2F_2^*(t)) + K_1(t)S_1K_1(t) \\ &\quad - (Q_1 + F_2^{*\top}(t)R_{12}F_2^*(t)), \quad K_1(T) = Q_{1T} \end{aligned}$$

has a symmetric solution  $K_1(t)$  on  $[0, T]$ . The optimal control is  $u_1^*(t) = -R_1^{-1}B_1^\top K_1(t)x_1(t)$ , so  $F_1^*(t) = -R_1^{-1}B_1^\top K_1(t)$ .

Similarly,  $u_2^*(t)$  solves an LQR problem implying  $F_2^*(t) = -R_2^{-1}B_2^\top K_2(t)$  where  $K_2(t)$  satisfies:

$$\begin{aligned} \dot{K}_2(t) &= -(A + B_1F_1^*(t))^\top K_2(t) - K_2(t)(A + B_1F_1^*(t)) + K_2(t)S_2K_2(t) \\ &\quad - (Q_2 + F_1^{*\top}(t)R_{21}F_1^*(t)), \quad K_2(T) = Q_{2T} \end{aligned}$$

Substituting  $F_1^*(t)$ ,  $F_2^*(t)$  into the Riccati equations gives the coupled equations in the theorem statement.

Conversely, if these equations have symmetric solutions, the strategies  $u_i^*(t) = -R_i^{-1}B_i^\top K_i(t)x(t)$  form an equilibrium by Theorem 8.2. Uniqueness follows from the LQR problems having unique solutions. The costs  $J_i = x_0^\top K_i(0)x_0$  also follow from Theorem 8.2.  $\square$

### Back to Theorem 1:

Now for the zero-sum game, adding the coupled Riccati equations in Theorem 2 gives:

$$\begin{aligned} \dot{K}_1(t) + \dot{K}_2(t) &= -(K_1(t) + K_2(t))(A - S_1K_1(t) - S_2K_2(t)) \\ &\quad - (A - S_1K_1(t) - S_2K_2(t))^\top(K_1(t) + K_2(t)) \\ K_1(T) + K_2(T) &= 0 \end{aligned}$$

Since this game is zero-sum, the costs must satisfy  $J_1 + J_2 = 0$  for any equilibrium. The unique solution to the above Riccati equation is  $K_1(t) = -K_2(t)$ . Substituting this into the first Riccati equation in Theorem 2 gives:

$$\begin{aligned} \dot{K}(t) &= -A^\top K(t) - K(t)A + K(t)(S_1 - S_2)K(t) - Q \\ K(T) &= Q_T \end{aligned}$$

Where  $K(t) = K_1(t)$ . So the game has a linear feedback Nash equilibrium if and only if this single Riccati equation has a symmetric solution  $K(t)$  on  $[0, T]$ .

The equilibrium strategies are:

$$\begin{aligned} u_1^*(t) &= -R_1^{-1}B_1^\top K(t)x(t) \\ u_2^*(t) &= R_2^{-1}B_2^\top K(t)x(t) \end{aligned}$$

And the costs are  $J_1 = x_0^\top K(0)x_0$  and  $J_2 = -J_1 = -x_0^\top K(0)x_0$ .

jjjjjjjjjjjj

**Proof of Theorem 1 (Zero-sum differential game):**

Consider the zero-sum differential game described by:

$$\dot{x}(t) = Ax(t) + B_1u_1(t) + B_2u_2(t), \quad x(0) = x_0$$

With cost functions:

$$\begin{aligned} J_1(u_1, u_2) &= \int_0^T \{x^\top(t)Qx(t) + u_1^\top(t)R_1u_1(t) - u_2^\top(t)R_2u_2(t)\} dt + x^\top(T)Q_Tx(T) \\ J_2(u_1, u_2) &= -J_1(u_1, u_2) \end{aligned}$$

Where  $Q, Q_T$  are symmetric, and  $R_1, R_2$  are positive definite.

To prove this theorem, we will first prove Theorem 2:

**Theorem 5** *The two-player linear quadratic differential game has, for every initial state, a linear feedback Nash equilibrium if and only if the following coupled Riccati equations have a set of symmetric solutions  $K_1(t), K_2(t)$  on  $[0, T]$ :*

$$\begin{aligned} \dot{K}_1(t) &= -(A - S_2K_2(t))^\top K_1(t) - K_1(t)(A - S_2K_2(t)) + K_1(t)S_1K_1(t) - Q_1 - K_2(t)S_{21}K_2(t) \\ K_1(T) &= Q_{1T} \end{aligned}$$

$$\begin{aligned} \dot{K}_2(t) &= -(A - S_1K_1(t))^\top K_2(t) - K_2(t)(A - S_1K_1(t)) + K_2(t)S_2K_2(t) - Q_2 - K_1(t)S_{12}K_1(t) \\ K_2(T) &= Q_{2T} \end{aligned}$$

Moreover, the equilibrium actions are:

$$\begin{aligned} u_1^*(t) &= -R_1^{-1}B_1^\top K_1(t)x(t) \\ u_2^*(t) &= -R_2^{-1}B_2^\top K_2(t)x(t) \end{aligned}$$

And the costs incurred are  $J_1 = x_0^\top K_1(0)x_0$ ,  $J_2 = x_0^\top K_2(0)x_0$ .

*Proof:* Assume  $u_i^*(t) = F_i^*(t)x(t)$ ,  $t \in [0, T]$ ,  $i = 1, 2$ , is a linear feedback equilibrium. Then by definition of linear feedback equilibrium,  $u_1^*(t)$  solves the LQR problem:

$$\begin{aligned} &\text{minimize } \int_0^T \{x_1^\top(s)(Q_1 + F_2^{*\top}(s)R_{12}F_2^*(s))x_1(s) + u_1^\top(s)R_1u_1(s)\} ds + x_1^\top(T)Q_{1T}x_1(T) \\ &\text{subject to } \dot{x}_1(t) = (A + B_2F_2^*(t))x_1(t) + B_1u_1(t), \quad x_1(0) = x_0 \end{aligned}$$

By Theorem 5.1, this has a solution if and only if the Riccati equation:

$$\begin{aligned} \dot{K}_1(t) &= -(A + B_2F_2^*(t))^\top K_1(t) - K_1(t)(A + B_2F_2^*(t)) + K_1(t)S_1K_1(t) \\ &\quad - (Q_1 + F_2^{*\top}(t)R_{12}F_2^*(t)), \quad K_1(T) = Q_{1T} \end{aligned}$$

has a symmetric solution  $K_1(t)$  on  $[0, T]$ . The optimal control is  $u_1^*(t) = -R_1^{-1}B_1^\top K_1(t)x_1(t)$ , so  $F_1^*(t) = -R_1^{-1}B_1^\top K_1(t)$ .

Similarly,  $u_2^*(t)$  solves an LQR problem implying  $F_2^*(t) = -R_2^{-1}B_2^\top K_2(t)$  where  $K_2(t)$  satisfies:

$$\begin{aligned}\dot{K}_2(t) &= -(A + B_1 F_1^*(t))^\top K_2(t) - K_2(t)(A + B_1 F_1^*(t)) + K_2(t)S_2 K_2(t) \\ &\quad - (Q_2 + F_1^{*\top}(t)R_{21}F_1^*(t)), \quad K_2(T) = Q_{2T}\end{aligned}$$

Substituting  $F_1^*(t)$ ,  $F_2^*(t)$  into the Riccati equations gives the coupled equations in the theorem statement.

Conversely, if these equations have symmetric solutions, the strategies  $u_i^*(t) = -R_i^{-1}B_i^\top K_i(t)x(t)$  form an equilibrium by Theorem 8.2. Uniqueness follows from the LQR problems having unique solutions. The costs  $J_i = x_0^\top K_i(0)x_0$  also follow from Theorem 8.2.  $\square$

Now, for the zero-sum game, adding the coupled Riccati equations in Theorem 2 gives:

$$\begin{aligned}\dot{K}_1(t) + \dot{K}_2(t) &= -(K_1(t) + K_2(t))(A - S_1 K_1(t) - S_2 K_2(t)) \\ &\quad - (A - S_1 K_1(t) - S_2 K_2(t))^\top(K_1(t) + K_2(t)) \\ K_1(T) + K_2(T) &= 0\end{aligned}$$

Since this game is zero-sum, the costs must satisfy  $J_1 + J_2 = 0$  for any equilibrium. The unique solution to the above Riccati equation is  $K_1(t) = -K_2(t)$ . Substituting this into the first Riccati equation in Theorem 2 gives:

$$\begin{aligned}\dot{K}(t) &= -A^\top K(t) - K(t)A + K(t)(S_1 - S_2)K(t) - Q \\ K(T) &= Q_T\end{aligned}$$

Where  $K(t) = K_1(t)$ . So the game has a linear feedback Nash equilibrium if and only if this single Riccati equation has a symmetric solution  $K(t)$  on  $[0, T]$ .

The equilibrium strategies are:

$$\begin{aligned}u_1^*(t) &= -R_1^{-1}B_1^\top K(t)x(t) \\ u_2^*(t) &= R_2^{-1}B_2^\top K(t)x(t)\end{aligned}$$

And the costs are  $J_1 = x_0^\top K(0)x_0$  and  $J_2 = -J_1 = -x_0^\top K(0)x_0$ .  $\square$

## Appendix C. Proof of Theorem 1: Zero-sum Differential Game

Consider the zero-sum differential game described by:

$$\dot{x}(t) = Ax(t) + B_1 u_1(t) + B_2 u_2(t), \quad x(0) = x_0$$

With cost functions:

$$\begin{aligned}J_1(u_1, u_2) &= \int_0^T \{x^\top(t)Qx(t) + u_1^\top(t)R_1 u_1(t) - u_2^\top(t)R_2 u_2(t)\} dt + x^\top(T)Q_T x(T) \\ J_2(u_1, u_2) &= -J_1(u_1, u_2)\end{aligned}$$

where  $Q$ ,  $Q_T$  are symmetric, and  $R_1$ ,  $R_2$  are positive definite.

**Theorem 6** *The two-player linear quadratic differential game has, for every initial state, a linear feedback Nash equilibrium if and only if the following coupled Riccati equations have a set of symmetric solutions  $K_1(t)$ ,  $K_2(t)$  on  $[0, T]$ :*

$$\begin{aligned}\dot{K}_1(t) &= -(A - S_2 K_2(t))^\top K_1(t) - K_1(t)(A - S_2 K_2(t)) + K_1(t)S_1 K_1(t) - Q_1 - K_2(t)S_{21} K_2(t) \\ K_1(T) &= Q_{1T}\end{aligned}$$

$$\begin{aligned}\dot{K}_2(t) &= -(A - S_1 K_1(t))^\top K_2(t) - K_2(t)(A - S_1 K_1(t)) + K_2(t)S_2 K_2(t) - Q_2 - K_1(t)S_{12} K_1(t) \\ K_2(T) &= Q_{2T}\end{aligned}$$

Moreover, the equilibrium actions are:

$$\begin{aligned}u_1^*(t) &= -R_1^{-1} B_1^\top K_1(t)x(t) \\ u_2^*(t) &= -R_2^{-1} B_2^\top K_2(t)x(t)\end{aligned}$$

And the costs incurred are  $J_1 = x_0^\top K_1(0)x_0$ ,  $J_2 = x_0^\top K_2(0)x_0$ .

Assume  $u_i^*(t) = F_i^*(t)x(t)$ ,  $t \in [0, T]$ ,  $i = 1, 2$ , is a linear feedback equilibrium. Then by definition of linear feedback equilibrium,  $u_1^*(t)$  solves the LQR problem:

$$\begin{aligned}&\text{minimize } \int_0^T \{x_1^\top(s)(Q_1 + F_2^{*\top}(s)R_{12}F_2^*(s))x_1(s) + u_1^\top(s)R_1 u_1(s)\} ds + x_1^\top(T)Q_{1T}x_1(T) \\ &\text{subject to } \dot{x}_1(t) = (A + B_2 F_2^*(t))x_1(t) + B_1 u_1(t), \quad x_1(0) = x_0\end{aligned}$$

By Theorem 5.1, this has a solution if and only if the Riccati equation:

$$\begin{aligned}\dot{K}_1(t) &= -(A + B_2 F_2^*(t))^\top K_1(t) - K_1(t)(A + B_2 F_2^*(t)) + K_1(t)S_1 K_1(t) \\ &\quad - (Q_1 + F_2^{*\top}(t)R_{12}F_2^*(t)), \quad K_1(T) = Q_{1T}\end{aligned}$$

has a symmetric solution  $K_1(t)$  on  $[0, T]$ . The optimal control is  $u_1^*(t) = -R_1^{-1} B_1^\top K_1(t)x_1(t)$ , so  $F_1^*(t) = -R_1^{-1} B_1^\top K_1(t)$ .

Similarly,  $u_2^*(t)$  solves an LQR problem implying  $F_2^*(t) = -R_2^{-1} B_2^\top K_2(t)$  where  $K_2(t)$  satisfies:

$$\begin{aligned}\dot{K}_2(t) &= -(A + B_1 F_1^*(t))^\top K_2(t) - K_2(t)(A + B_1 F_1^*(t)) + K_2(t)S_2 K_2(t) \\ &\quad - (Q_2 + F_1^{*\top}(t)R_{21}F_1^*(t)), \quad K_2(T) = Q_{2T}\end{aligned}$$

Substituting  $F_1^*(t)$ ,  $F_2^*(t)$  into the Riccati equations gives the coupled equations in the theorem statement.  
mmmmmmmmmmmm

**Proof of Theorem 1 (Zero-sum differential game):**

Consider the zero-sum differential game described by:

$$\dot{x}(t) = Ax(t) + B_1 u_1(t) + B_2 u_2(t), \quad x(0) = x_0$$

With cost functions:

$$J_1(u_1, u_2) = \int_0^T \{x^\top(t)Qx(t) + u_1^\top(t)R_1u_1(t) - u_2^\top(t)R_2u_2(t)\} dt + x^\top(T)Q_Tx(T)$$

$$J_2(u_1, u_2) = -J_1(u_1, u_2)$$

Where  $Q, Q_T$  are symmetric, and  $R_1, R_2$  are positive definite.

**Theorem 7** *The two-player linear quadratic differential game has, for every initial state, a linear feedback Nash equilibrium if and only if the following coupled Riccati equations have a set of symmetric solutions  $K_1(t), K_2(t)$  on  $[0, T]$ :*

$$\dot{K}_1(t) = -(A - S_2K_2(t))^\top K_1(t) - K_1(t)(A - S_2K_2(t)) + K_1(t)S_1K_1(t) - Q_1 - K_2(t)S_{21}K_2(t)$$

$$K_1(T) = Q_{1T}$$

$$\dot{K}_2(t) = -(A - S_1K_1(t))^\top K_2(t) - K_2(t)(A - S_1K_1(t)) + K_2(t)S_2K_2(t) - Q_2 - K_1(t)S_{12}K_1(t)$$

$$K_2(T) = Q_{2T}$$

Moreover, the equilibrium actions are:

$$u_1^*(t) = -R_1^{-1}B_1^\top K_1(t)x(t)$$

$$u_2^*(t) = -R_2^{-1}B_2^\top K_2(t)x(t)$$

And the costs incurred are  $J_1 = x_0^\top K_1(0)x_0$ ,  $J_2 = x_0^\top K_2(0)x_0$ .

*Proof:*. Assume  $u_i^*(t) = F_i^*(t)x(t)$ ,  $t \in [0, T]$ ,  $i = 1, 2$ , is a linear feedback equilibrium. Then by definition of linear feedback equilibrium,  $u_1^*(t)$  solves the LQR problem:

$$\text{minimize } \int_0^T \{x_1^\top(s)(Q_1 + F_2^{*\top}(s)R_{12}F_2^*(s))x_1(s) + u_1^\top(s)R_1u_1(s)\} ds + x_1^\top(T)Q_{1T}x_1(T)$$

$$\text{subject to } \dot{x}_1(t) = (A + B_2F_2^*(t))x_1(t) + B_1u_1(t), \quad x_1(0) = x_0$$

By Theorem 5.1, this has a solution if and only if the Riccati equation:

$$\dot{K}_1(t) = -(A + B_2F_2^*(t))^\top K_1(t) - K_1(t)(A + B_2F_2^*(t)) + K_1(t)S_1K_1(t)$$

$$- (Q_1 + F_2^{*\top}(t)R_{12}F_2^*(t)), \quad K_1(T) = Q_{1T}$$

has a symmetric solution  $K_1(t)$  on  $[0, T]$ . The optimal control is  $u_1^*(t) = -R_1^{-1}B_1^\top K_1(t)x_1(t)$ , so  $F_1^*(t) = -R_1^{-1}B_1^\top K_1(t)$ .

Similarly,  $u_2^*(t)$  solves an LQR problem implying  $F_2^*(t) = -R_2^{-1}B_2^\top K_2(t)$  where  $K_2(t)$  satisfies:

$$\dot{K}_2(t) = -(A + B_1F_1^*(t))^\top K_2(t) - K_2(t)(A + B_1F_1^*(t)) + K_2(t)S_2K_2(t)$$

$$- (Q_2 + F_1^{*\top}(t)R_{21}F_1^*(t)), \quad K_2(T) = Q_{2T}$$

Substituting  $F_1^*(t), F_2^*(t)$  into the Riccati equations gives the coupled equations in the theorem statement.

Conversely, if these equations have symmetric solutions, the strategies  $u_i^*(t) = -R_i^{-1}B_i^\top K_i(t)x(t)$  form an equilibrium by Theorem 8.2. Uniqueness follows from the LQR problems having unique solutions. The costs  $J_i = x_0^\top K_i(0)x_0$  also follow from Theorem 8.2.  $\square$

Now, for the zero-sum game, adding the coupled Riccati equations in Theorem 2 gives:

$$\begin{aligned}\dot{K}_1(t) + \dot{K}_2(t) &= -(K_1(t) + K_2(t))(A - S_1 K_1(t) - S_2 K_2(t)) \\ &\quad - (A - S_1 K_1(t) - S_2 K_2(t))^\top (K_1(t) + K_2(t)) \\ K_1(T) + K_2(T) &= 0\end{aligned}$$

Since this game is zero-sum, the costs must satisfy  $J_1 + J_2 = 0$  for any equilibrium. The unique solution to the above Riccati equation is  $K_1(t) = -K_2(t)$ . Substituting this into the first Riccati equation in Theorem 2 gives:

$$\begin{aligned}\dot{K}(t) &= -A^\top K(t) - K(t)A + K(t)(S_1 - S_2)K(t) - Q \\ K(T) &= Q_T\end{aligned}$$

Where  $K(t) = K_1(t)$ . So the game has a linear feedback Nash equilibrium if and only if this single Riccati equation has a symmetric solution  $K(t)$  on  $[0, T]$ .

The equilibrium strategies are:

$$\begin{aligned}u_1^*(t) &= -R_1^{-1}B_1^\top K(t)x(t) \\ u_2^*(t) &= R_2^{-1}B_2^\top K(t)x(t)\end{aligned}$$

And the costs are  $J_1 = x_0^\top K(0)x_0$  and  $J_2 = -J_1 = -x_0^\top K(0)x_0$ .

### Proof of Theorem 1 (Zero-sum differential game):

Consider the zero-sum differential game described by:

$$\dot{x}(t) = Ax(t) + B_1u_1(t) + B_2u_2(t), \quad x(0) = x_0$$

With cost functions:

$$\begin{aligned}J_1(u_1, u_2) &= \int_0^T \{x^\top(t)Qx(t) + u_1^\top(t)R_1u_1(t) - u_2^\top(t)R_2u_2(t)\} dt + x^\top(T)Q_Tx(T) \\ J_2(u_1, u_2) &= -J_1(u_1, u_2)\end{aligned}$$

Where  $Q, Q_T$  are symmetric, and  $R_1, R_2$  are positive definite.

**Definition 1** A linear feedback Nash equilibrium for this game consists of control policies  $u_1^*(t)$  and  $u_2^*(t)$  such that no player can improve their cost by unilaterally changing their control policy.

**Theorem 8** The zero-sum differential game described above has a linear feedback Nash equilibrium if and only if the following coupled Riccati equations have a set of symmetric solutions  $K_1(t), K_2(t)$  on  $[0, T]$ :

$$\begin{aligned}\dot{K}_1(t) &= -(A - S_2 K_2(t))^\top K_1(t) - K_1(t)(A - S_2 K_2(t)) + K_1(t)S_1 K_1(t) - Q_1 - K_2(t)S_{21} K_2(t) \\ K_1(T) &= Q_{1T}\end{aligned}$$

$$\begin{aligned}\dot{K}_2(t) &= -(A - S_1 K_1(t))^\top K_2(t) - K_2(t)(A - S_1 K_1(t)) + K_2(t)S_2 K_2(t) - Q_2 - K_1(t)S_{12} K_1(t) \\ K_2(T) &= Q_{2T}\end{aligned}$$

Moreover, the equilibrium actions are:

$$\begin{aligned}u_1^*(t) &= -R_1^{-1} B_1^\top K_1(t)x(t) \\ u_2^*(t) &= -R_2^{-1} B_2^\top K_2(t)x(t)\end{aligned}$$

And the costs incurred are  $J_1 = x_0^\top K_1(0)x_0$ ,  $J_2 = x_0^\top K_2(0)x_0$ .

*Proof.*: Assume  $u_i^*(t) = F_i^*(t)x(t)$ ,  $t \in [0, T]$ ,  $i = 1, 2$ , is a linear feedback equilibrium. Then by definition of linear feedback equilibrium,  $u_1^*(t)$  solves the LQR problem:

$$\begin{aligned}&\text{minimize } \int_0^T \{x_1^\top(s)(Q_1 + F_2^{*\top}(s)R_{12}F_2^*(s))x_1(s) + u_1^\top(s)R_1 u_1(s)\} ds + x_1^\top(T)Q_{1T}x_1(T) \\ &\text{subject to } \dot{x}_1(t) = (A + B_2 F_2^*(t))x_1(t) + B_1 u_1(t), \quad x_1(0) = x_0\end{aligned}$$

By Theorem 1, this has a solution if and only if the Riccati equation:

$$\begin{aligned}\dot{K}_1(t) &= -(A + B_2 F_2^*(t))^\top K_1(t) - K_1(t)(A + B_2 F_2^*(t)) + K_1(t)S_1 K_1(t) \\ &\quad - (Q_1 + F_2^{*\top}(t)R_{12}F_2^*(t)), \quad K_1(T) = Q_{1T}\end{aligned}$$

has a symmetric solution  $K_1(t)$  on  $[0, T]$ . The optimal control is  $u_1^*(t) = -R_1^{-1} B_1^\top K_1(t)x_1(t)$ , so  $F_1^*(t) = -R_1^{-1} B_1^\top K_1(t)$ .

Similarly,  $u_2^*(t)$  solves an LQR problem implying  $F_2^*(t) = -R_2^{-1} B_2^\top K_2(t)$  where  $K_2(t)$  satisfies:

$$\begin{aligned}\dot{K}_2(t) &= -(A + B_1 F_1^*(t))^\top K_2(t) - K_2(t)(A + B_1 F_1^*(t)) + K_2(t)S_2 K_2(t) \\ &\quad - (Q_2 + F_1^{*\top}(t)R_{21}F_1^*(t)), \quad K_2(T) = Q_{2T}\end{aligned}$$

Substituting  $F_1^*(t)$ ,  $F_2^*(t)$  into the Riccati equations gives the coupled equations in Theorem 1.

Conversely, if these equations have symmetric solutions, the strategies  $u_i^*(t) = -R_i^{-1} B_i^\top K_i(t)x(t)$  form an equilibrium by Theorem 1. Uniqueness follows from the LQR problems having unique solutions. The costs  $J_i = x_0^\top K_i(0)x_0$  also follow from Theorem 1.  $\square$

Now, for the zero-sum game, adding the coupled Riccati equations gives:

$$\begin{aligned}\dot{K}_1(t) + \dot{K}_2(t) &= -(K_1(t) + K_2(t))(A - S_1 K_1(t) - S_2 K_2(t)) \\ &\quad - (A - S_1 K_1(t) - S_2 K_2(t))^\top(K_1(t) + K_2(t)) \\ K_1(T) + K_2(T) &= 0\end{aligned}$$

Since this game is zero-sum, the costs must satisfy  $J_1 + J_2 = 0$  for any equilibrium. The unique solution to the above Riccati equation is  $K_1(t) = -K_2(t)$ . Substituting this into the first Riccati equation gives:

$$\begin{aligned}\dot{K}(t) &= -A^\top K(t) - K(t)A + K(t)(S_1 - S_2)K(t) - Q \\ K(T) &= Q_T\end{aligned}$$

Where  $K(t) = K_1(t)$ . So the game has a linear feedback Nash equilibrium if and only if this single Riccati equation has a symmetric solution  $K(t)$  on  $[0, T]$ .

The equilibrium strategies are:

$$\begin{aligned} u_1^*(t) &= -R_1^{-1}B_1^\top K(t)x(t) \\ u_2^*(t) &= R_2^{-1}B_2^\top K(t)x(t) \end{aligned}$$

And the costs are  $J_1 = x_0^\top K(0)x_0$  and  $J_2 = -J_1 = -x_0^\top K(0)x_0$ .

### Proof of Theorem 1 (Zero-sum differential game):

Consider the zero-sum differential game described by:

$$\dot{x}(t) = Ax(t) + B_1u_1(t) + B_2u_2(t), \quad x(0) = x_0$$

With cost functions:

$$\begin{aligned} J_1(u_1, u_2) &= \int_0^T \{x^\top(t)Qx(t) + u_1^\top(t)R_1u_1(t) - u_2^\top(t)R_2u_2(t)\} dt + x^\top(T)Q_Tx(T) \\ J_2(u_1, u_2) &= -J_1(u_1, u_2) \end{aligned}$$

Where  $Q, Q_T$  are symmetric, and  $R_1, R_2$  are positive definite.

**Definition 2** A linear feedback Nash equilibrium for this game consists of control policies  $u_1^*(t)$  and  $u_2^*(t)$  such that no player can improve their cost by unilaterally changing their control policy.

**Theorem 9** The zero-sum differential game described above has a linear feedback Nash equilibrium if and only if the following coupled Riccati equations have a set of symmetric solutions  $K_1(t), K_2(t)$  on  $[0, T]$ :

$$\begin{aligned} \dot{K}_1(t) &= -(A - S_2K_2(t))^\top K_1(t) - K_1(t)(A - S_2K_2(t)) + K_1(t)S_1K_1(t) - Q_1 - K_2(t)S_{21}K_2(t) \\ K_1(T) &= Q_{1T} \end{aligned}$$

$$\begin{aligned} \dot{K}_2(t) &= -(A - S_1K_1(t))^\top K_2(t) - K_2(t)(A - S_1K_1(t)) + K_2(t)S_2K_2(t) - Q_2 - K_1(t)S_{12}K_1(t) \\ K_2(T) &= Q_{2T} \end{aligned}$$

Moreover, the equilibrium actions are:

$$\begin{aligned} u_1^*(t) &= -R_1^{-1}B_1^\top K_1(t)x(t) \\ u_2^*(t) &= -R_2^{-1}B_2^\top K_2(t)x(t) \end{aligned}$$

And the costs incurred are  $J_1 = x_0^\top K_1(0)x_0$ ,  $J_2 = x_0^\top K_2(0)x_0$ .

*Proof:* Assume  $u_i^*(t) = F_i^*(t)x(t)$ ,  $t \in [0, T]$ ,  $i = 1, 2$ , is a linear feedback equilibrium. Then by definition of linear feedback equilibrium,  $u_1^*(t)$  solves the LQR problem:

$$\begin{aligned} & \text{minimize } \int_0^T \{x_1^\top(s)(Q_1 + F_2^{*\top}(s)R_{12}F_2^*(s))x_1(s) + u_1^\top(s)R_1u_1(s)\} ds + x_1^\top(T)Q_{1T}x_1(T) \\ & \text{subject to } \dot{x}_1(t) = (A + B_2F_2^*(t))x_1(t) + B_1u_1(t), \quad x_1(0) = x_0 \end{aligned}$$

By Theorem 1, this has a solution if and only if the Riccati equation:

$$\begin{aligned} \dot{K}_1(t) &= -(A + B_2F_2^*(t))^\top K_1(t) - K_1(t)(A + B_2F_2^*(t)) + K_1(t)S_1K_1(t) \\ &\quad - (Q_1 + F_2^{*\top}(t)R_{12}F_2^*(t)), \quad K_1(T) = Q_{1T} \end{aligned}$$

has a symmetric solution  $K_1(t)$  on  $[0, T]$ . The optimal control is  $u_1^*(t) = -R_1^{-1}B_1^\top K_1(t)x_1(t)$ , so  $F_1^*(t) = -R_1^{-1}B_1^\top K_1(t)$ .

Similarly,  $u_2^*(t)$  solves an LQR problem implying  $F_2^*(t) = -R_2^{-1}B_2^\top K_2(t)$  where  $K_2(t)$  satisfies:

$$\begin{aligned} \dot{K}_2(t) &= -(A + B_1F_1^*(t))^\top K_2(t) - K_2(t)(A + B_1F_1^*(t)) + K_2(t)S_2K_2(t) \\ &\quad - (Q_2 + F_1^{*\top}(t)R_{21}F_1^*(t)), \quad K_2(T) = Q_{2T} \end{aligned}$$

Substituting  $F_1^*(t)$ ,  $F_2^*(t)$  into the Riccati equations gives the coupled equations in Theorem 1.

Conversely, if these equations have symmetric solutions, the strategies  $u_i^*(t) = -R_i^{-1}B_i^\top K_i(t)x(t)$  form an equilibrium by Theorem 1. Uniqueness follows from the LQR problems having unique solutions. The costs  $J_i = x_0^\top K_i(0)x_0$  also follow from Theorem 1.  $\square$

Now, for the zero-sum game, adding the coupled Riccati equations gives:

$$\begin{aligned} \dot{K}_1(t) + \dot{K}_2(t) &= -(K_1(t) + K_2(t))(A - S_1K_1(t) - S_2K_2(t)) \\ &\quad - (A - S_1K_1(t) - S_2K_2(t))^\top(K_1(t) + K_2(t)) \\ K_1(T) + K_2(T) &= 0 \end{aligned}$$

Since this game is zero-sum, the costs must satisfy  $J_1 + J_2 = 0$  for any equilibrium. The unique solution to the above Riccati equation is  $K_1(t) = -K_2(t)$ . Substituting this into the first Riccati equation gives:

$$\begin{aligned} \dot{K}(t) &= -A^\top K(t) - K(t)A + K(t)(S_1 - S_2)K(t) - Q \\ K(T) &= Q_T \end{aligned}$$

Where  $K(t) = K_1(t)$ . So the game has a linear feedback Nash equilibrium if and only if this single Riccati equation has a symmetric solution  $K(t)$  on  $[0, T]$ .

The equilibrium strategies are:

$$\begin{aligned} u_1^*(t) &= -R_1^{-1}B_1^\top K(t)x(t) \\ u_2^*(t) &= R_2^{-1}B_2^\top K(t)x(t) \end{aligned}$$

And the costs are  $J_1 = x_0^\top K(0)x_0$  and  $J_2 = -J_1 = -x_0^\top K(0)x_0$ .